
Improving Offline RL by Blending Heuristics

Sinong Geng
Princeton University
Princeton, NJ

Aldo Pacchiano
Microsoft Research
New York City, NY

Andrey Kolobov
Microsoft Research
Redmond, WA

Ching-An Cheng
Microsoft Research
Redmond, WA

Abstract

We propose **Heuristic Blending** (HUBL), a simple performance-improving technique for a broad class of offline RL algorithms based on value bootstrapping. HUBL modifies Bellman operators used in these algorithms, partially replacing the bootstrapped values with Monte-Carlo returns as heuristics. For trajectories with higher returns, HUBL relies more on heuristics and less on bootstrapping; otherwise, it leans more heavily on bootstrapping. We show that this idea can be easily implemented by relabeling the offline datasets with adjusted rewards and discount factors, making HUBL readily usable by many existing offline RL implementations. We theoretically prove that HUBL reduces offline RL’s complexity and thus improves its finite-sample performance. Furthermore, we empirically demonstrate that HUBL consistently improves the policy quality of four state-of-the-art bootstrapping-based offline RL algorithms (ATAC, CQL, TD3+BC, and IQL), by 9% on average over 27 datasets of the D4RL and Meta-World benchmarks.

1 Introduction

Offline reinforcement learning (RL) aims to learn decision-making strategies from static logged datasets [Fujimoto et al., 2019, Lange et al., 2012]. It has attracted increased interest in recent years, with the availability of large offline datasets being on the rise and online exploration required by alternative approaches such as online RL [Sutton and Barto, 2018] remaining expensive and risky in many real-world applications, such as robotics and healthcare.

Among offline RL algorithms, model-free approaches using dynamic programming with value bootstrapping have demonstrated particularly strong performance, achieving state-of-the-art (SoTA) results in offline RL benchmarks [Fu et al., 2020, Gulcehre et al., 2020]. The commonly used CQL [Kumar et al., 2020], TD3+BC [Fujimoto and Gu, 2021], IQL [Kostrikov et al., 2022], and ATAC [Cheng et al., 2022] belong to this category. They follow the actor-critic scheme and adopt the principle of pessimism in the face of uncertainty to optimize an agent via a performance lower bound that penalizes taking unfamiliar actions. Despite their strengths, existing model-free offline RL methods also have a major weakness: they do not perform *consistently*. An algorithm that does well on one dataset may struggle on another, sometimes even underperforming behavior cloning [Dulac-Arnold et al., 2021, Kumar et al., 2019, Sutton and Barto, 2018]. These performance fluctuations stand in the way of applying even the strongest offline RL approaches to practical problems.

In this work, we propose **Heuristic Blending** (HUBL), an easy-to-implement technique to address offline RL’s performance inconsistency. HUBL operates *in combination with* a bootstrapping-based offline RL algorithm by using heuristic value estimates to modify the rewards and discounts in the dataset that the base offline RL algorithm consumes. Effectively, this modification blends heuristic

values into dynamic programming to partially replace bootstrapping. Relying less on bootstrapping alleviates potential issues that bootstrapping causes and helps achieve more stable performance.

HUBL can be easily implemented as a data relabeling procedure as summarized in Figure 1. Thus, it is readily applicable to many existing offline RL methods. Specifically, combining HUBL with an offline RL algorithm amounts to running this algorithm on a relabeled version of the original dataset with modified rewards \tilde{r} and discounts $\tilde{\gamma}$:

$$\tilde{r} = r + \gamma\lambda h, \quad \tilde{\gamma} = \gamma(1 - \lambda),$$

where r is blended with a heuristic h , $\tilde{\gamma}$ is the reduced discount, and $\lambda \in [0, 1]$ is a blending factor representing the degree of trust towards the heuristic. We set h to be the Monte-Carlo returns of the trajectories in the dataset for offline RL. Such a heuristic is efficient and stable to compute, unlike bootstrapped Q -value estimates. The blending factor λ in HUBL can be trajectory-dependent. Intuitively, we want λ to be large (relying more on the heuristic) at trajectories where the behavior policy that collected the dataset performs well, and small (relying more on bootstrapped Q -values) otherwise. We provide three practical designs for λ ; they use only one hyperparameter, which, empirically, does not need active tuning.

We analyze HUBL’s performance both theoretically and empirically. Theoretically, we provide a finite-sample performance bound for offline RL with HUBL by framing it as solving a reshaped Markov decision process (MDP). To our knowledge, this is the first theoretical result for RL with heuristics in the *offline* setting. Our analysis shows that HUBL performs a bias-regret trade-off. On the one hand, solving the reshaped MDP with a smaller discount factor requires less bootstrapping and is relatively “easier”, so the regret is smaller. On the other hand, HUBL induces bias due to reshaping the original MDP. Nonetheless, we demonstrate that the bias can be controlled by setting the λ factor based on the above intuition, allowing HUBL to improve the performance of the base offline RL method.

Empirically, we run HUBL with the four aforementioned offline RL methods – CQL, TD3+BC, IQL, and ATAC – and show that enhancing these SoTA algorithms with HUBL can improve their performance by 9% on average across 27 datasets of D4RL [Fu et al., 2020] and Meta-World [Yu et al., 2020]. Notably, in some datasets where the base offline RL method shows inconsistent performance, HUBL can achieve more than 50% relative performance improvement.

2 Related Work

Bootstrapping-based Offline RL A fundamental challenge of bootstrapping-based offline RL is the *deadly triad* [Sutton and Barto, 2018]: a negative interference between 1) off-policy learning from data with limited support, 2) value bootstrapping, and 3) the function approximator. Modern offline RL algorithms such as CQL [Kumar et al., 2020], TD3+BC [Fujimoto and Gu, 2021], IQL [Kostrikov et al., 2022], ATAC [Cheng et al., 2022], PEVI [Jin et al., 2021], and VI-LCB [Rashidinejad et al., 2021] employ pessimism to discourage the agent from taking actions unsupported by the data, which has proved to be an effective strategy to address the issue of limited support. However, they still suffer from a combination of errors in bootstrapping and function approximation. HUBL aims to address this with stable-to-compute Monte-Carlo return heuristics and thus is a *complementary* technique to pessimism.

RL by blending multi-step returns The idea of blending multi-step Monte-Carlo returns into the bootstrapping operator to reduce the degree of bootstrapping and thereby increase its performance has a long history in RL. This technique has been widely used in temporal difference methods [Sutton and Barto, 2018], where the blending is achieved by modifying gradient updates [Jiang et al., 2021, Seijen and Sutton, 2014, Sutton et al., 2016] and reweighting observations [Imani et al., 2018]. It has also been applied to improve Q function estimation [Wright et al., 2013], online exploration [Bellemare

Algorithm 1 Base offline RL method

- 1: **Input:** data $\mathbb{D} = \{(s, a, s', r, \gamma)\}$
 - 2: **for** each iteration **do**
 - 3: Sample $(s, a, r, s', \gamma) \in \mathbb{D}$
 - 4: Dynamic Programming update using (s, a, r, s', γ)
 - 5: **end for**
-



Algorithm 2 HUBL + Offline RL

- 1: **Input:** data $\mathbb{D} = \{(s, a, s', r, \gamma)\}$
 - 2: $\tilde{\mathbb{D}} \leftarrow$ Relabel \mathbb{D} with modified rewards \tilde{r} & discounts $\tilde{\gamma}$ using heuristics h
 - 3: **for** each iteration **do**
 - 4: Sample $(s, a, \tilde{r}, s', \tilde{\gamma}) \in \tilde{\mathbb{D}}$
 - 5: Dynamic Programming update using $(s, a, \tilde{r}, s', \tilde{\gamma})$
 - 6: **end for**
-

Figure 1: HUBL overview

et al., 2016, Ostrovski et al., 2017] and the sensitivity to model misspecification [Zanette et al., 2021], and is especially effective for sparse-reward problems Wilcox et al. [2022]. In contrast to most of the aforementioned works, which focus on blending Monte-Carlo returns as part of an RL algorithm’s *online* operation, HUBL is designed for the *offline* setting and acts as a simple data relabeling step. Recently, Wilcox et al. [2022] have also proposed the idea of data relabeling, but their design takes a max of multi-step returns and bootstrapped values and as a result tends to overestimate Q -functions. We observed this to be detrimental when data has a limited support.

RL with heuristics More generally, HUBL relates to the framework of blending heuristics (which might be estimating quantities other than a policy’s value) into bootstrapping [Bejjani et al., 2018, Cheng et al., 2021, Hoeller et al., 2020, Zhong et al., 2013]. However, the existing results focus only on the online case and do not conclusively show whether blending heuristics is valid in the offline case. For instance, the theoretical analysis in Cheng et al. [2021] breaks when applied to the offline setting as we will demonstrate in Section 5. The major difference is that online approaches rely heavily on collecting new data with the learned policy, which is impossible in the offline case. In this paper, we employ a novel analysis technique to demonstrate that blending heuristics is effective even in offline RL. To the best of our knowledge, ours is the first work to extend heuristic blending to the offline setting with both rigorous theoretical analysis and empirical results demonstrating performance improvement. One key insight is the adoption of a *trajectory-dependent* λ blending factor, which is both a performance-improving design as well as a novel analysis technicality. Our trajectory-dependent blending is inspired by unifying task specification in online RL [White, 2017], where the discount factor is transition-dependent.

Discount regularization HUBL modifies the reward with a heuristic and reduces the discount. Discount regularization, on the other hand, is a complexity reduction technique that reduces *only* the discount. The idea of simplifying decision-making problems by reducing discount factors can be traced back to Blackwell optimality in the known MDP setting [Blackwell, 1962]. Most existing results on discount regularization [Jiang et al., 2015, Petrik and Scherrer, 2008] study the MDP setting or the online RL setting [Van Seijen et al., 2019]. Recently, Hu et al. [2022] has shown that discount regularization can also reduce the complexity of offline RL and serve as an extra source of pessimism. However, as we will show, simply reducing the discount without the compensation of blending heuristics in the offline setting can be excessively pessimistic and introduce large bias that hurts performance. In Section 6.1, we rigorously analyze this bias and empirically demonstrate the advantages of HUBL over discount regularization.

3 Background

In this section, we define the problem setup of offline RL (Section 3.1), review dynamic programming with value bootstrapping and briefly survey methods using heuristics (Section 3.2).

3.1 Offline RL and Notation

We consider offline RL in a Markov decision process (MDP) $\mathcal{M} = (\mathcal{S}, \mathcal{A}, \mathcal{P}, r, \gamma)$, where \mathcal{S} denotes the state space, \mathcal{A} the action space, \mathcal{P} the transition function, $r : \mathcal{S} \times \mathcal{A} \rightarrow [0, 1]$ the reward function, and $\gamma \in [0, 1)$ the discount factor. A decision-making *policy* π is a mapping from \mathcal{S} to \mathcal{A} , and its *value function* is defined as $V^\pi(s) = \mathbb{E}[\sum_{t=0}^{\infty} \gamma^t r(s_t, a_t) | s_0 = s, a_t \sim \pi(\cdot | s_t)]$. In addition, we define $Q^\pi(s, a) := r(s, a) + \gamma \mathbb{E}_{s' \sim \mathcal{P} | s, a} [V^\pi(s')]$ as its state-action value function (i.e., Q function). We use V^* to denote the value function of the optimal policy π^* , which is our performance target. In addition, we introduce several definitions of distributions. First, we define the average state distribution of a policy π starting from an initial state s_0 as $d^\pi(s, a; s_0) := \sum_{t=0}^{\infty} d_t^\pi(s, a; s_0)$, where $d_t^\pi(s, a; s_0)$ is the state-action distribution at time t generated by running policy π from an initial state s_0 . We assume that the MDP starts with a fixed initial state distribution d_0 . With slight abuse of notation, we define the average state distribution starting from d_0 as $d^\pi(s, a) := d^\pi(s, a; d_0)$, and $d^\pi(s, a, s') := d^\pi(s, a) \mathcal{P}(s' | s, a)$.

The objective of offline RL is to learn a well-performing policy $\hat{\pi}$ while using a pre-collected offline dataset \mathbb{D} . The agent has no knowledge of the MDP \mathcal{M} except information contained in \mathbb{D} , and it cannot perform online interactions with environment to further collect data. We assume that the dataset $\mathbb{D} := \{\tau\}$ contains multiple trajectories collected by a *behavior policy*, where each $\tau = \{(s_t, a_t, r_t)\}_{t=1}^{T_\tau}$ denotes a trajectory with length T_τ . Suppose these trajectories contain N

transition tuples in total. With abuse of notation, we also write $\mathbb{D} := \{(s, a, s', r, \gamma)\}$, where states s and action a follow a distribution $\mu(s, a)$ induced by the behavior policy, s' is the state after each transition, r is the reward at s, a , and γ is the discount factor of the MDP. Note that the value of discount γ is the same in each tuple. We use Ω to denote the support of $\mu(s, a)$. *We do not make the full support assumption, in the sense that the dataset \mathbb{D} may not contain a tuple for every s, a, s' transition in the MDP.*

3.2 Dynamic Programming with Bootstrapping and Heuristics

Bootstrapping Many offline RL methods leverage dynamic programming with value bootstrapping. Given a policy π , we recall Q^π and V^π satisfy the Bellman equation:

$$Q^\pi(s, a) = r(s, a) + \overbrace{\gamma \mathbb{E}_{s' \sim \mathcal{P}(\cdot|s, a)} [V^\pi(s')]}^{(\text{bootstrapping})}. \quad (1)$$

These bootstrapping-based methods compute $Q^\pi(s, a)$ using an approximated version of (1): given sampled tuples (s, a, s', γ, r) , such methods minimize the difference between the two sides of (1) with both Q^π and V^π replaced with function approximators¹. With limited offline data, learning the function approximator using bootstrapping can be challenging and yields inconsistent performance across different datasets [Dulac-Arnold et al., 2021, Kumar et al., 2019, Sutton and Barto, 2018].

Heuristics A *heuristic* is a value function calculated using domain knowledge, Monte-Carlo averages, or pre-training. Heuristics are widely used in online RL, planning, and control to improve the performance of decision-making [Bejjani et al., 2018, Cheng et al., 2021, Hoeller et al., 2020, Zhong et al., 2013]. In this paper, we focus on the offline setting, and consider heuristics h that approximate the value function of the behavior policy. Such heuristics can be estimated from \mathbb{D} via Monte-Carlo methods.

4 Heuristic Blending (HUBL)

In this section we describe our main contribution — **Heuristic Blending (HUBL)**, an algorithm that works in combination with bootstrapping-based offline RL methods and improves their performance.

4.1 Motivation

HUBL uses a heuristic computed as the Monte-Carlo return of the behavior policy in the training dataset \mathbb{D} to improve offline RL. It reduces an offline RL algorithm’s bootstrapping at trajectories where the behavior policy performs well, i.e., where the value of the behavior policy (i.e. the heuristic value) is high. With less amount of bootstrapping, it mitigates bootstrapping-induced issues on convergence stability and performance. In addition, since the extent of blending between the heuristic and bootstrapping is trajectory-dependent, HUBL introduce only limited performance bias to the base algorithm, and therefore can improve its performance overall.

Algorithm 3 HUBL + Offline RL

- 1: **Input:** Dataset $\mathbb{D} = \{(s, a, s', r, \gamma)\}$
 - 2: Compute h_t for each trajectory in \mathbb{D}
 - 3: Compute λ_t for each trajectory in \mathbb{D}
 - 4: Relabel r & γ by h_t and λ_t as \tilde{r} and $\tilde{\gamma}$ and create $\tilde{\mathbb{D}} = \{(s, a, s', \tilde{r}, \tilde{\gamma})\}$
 - 5: $\hat{\pi} \leftarrow$ Offline RL on $\tilde{\mathbb{D}}$
-

4.2 Algorithm

As summarized in Algorithm 3, HUBL can be easily implemented: first relabel a base offline RL algorithm’s training dataset $\mathbb{D} = \{(s, a, s', r, \gamma)\}$ with modified rewards \tilde{r} and discount factors $\tilde{\gamma}$, creating a new dataset $\tilde{\mathbb{D}} := \{(s, a, s', \tilde{r}, \tilde{\gamma})\}$; next run the base algorithm on $\tilde{\mathbb{D}}$.

The data relabeling is done in three steps:

Step 0: As a preparation step, we convert the data tuples in \mathbb{D} back to trajectories like $\tau = \{(s_t, a_t, r_t)\}_{t=1}^{T_\tau}$. For the next two steps, we work on data trajectories instead of data tuples to compute heuristics and blending factors.

¹Q-learning-based offline RL in Kostrikov et al. [2022] uses a dynamic programming equation similar to (1) but with $V^\pi(s) = \arg \max_{a \in \mathcal{A}} Q^\pi(s, a)$.

Step 1: Computing heuristic h_t We compute heuristics by Monte-Carlo returns. For each $\tau = \{(s_t, a_t, r_t)\}_{t=1}^{T_\tau} \in \mathbb{D}$, we calculate the heuristics as² $h_t = \sum_{k=t}^{T_\tau} \gamma^{k-t} r_k$ and update the data trajectory as $\tau \leftarrow \{(s_t, a_t, r_t, h_t)\}_{t=1}^{T_\tau}$.

Step 2: Computing blending factor λ_t We append a scalar $\lambda_t = \lambda(\tau) \in [0, 1]$ at each time point t of each trajectory as the blending factor, leading to $\tau \leftarrow \{(s_t, a_t, r_t, h_t, \lambda_t)\}_{t=1}^{T_\tau}$. λ_t indicates the confidence in the heuristics on the trajectory. Intuitively, λ_t decides the contribution of heuristics over bootstrapped values in dynamic programming to update the Q -function. We desire λ_t to be closer to 1 when the heuristic value h_t is higher (i.e., at states where the heuristic is closer to the optimal Q -value) to make offline RL rely more on the heuristic, and λ_t closer to zero when heuristic is lower to make offline RL to use more bootstrapping. We experiment with three different designs of $\lambda(\tau)$:

- *Constant*: As a baseline, we consider $\lambda(\tau) = \alpha \in [0, 1]$ for all s . We show that, despite forcing the same heuristic weight for every state, this formulation already provides performance improvements.
- *Sigmoid*: As an alternative, we use the sigmoid function to construct a trajectory-dependent blending function $\lambda(\tau) = \alpha \sigma(\sum_{t=1}^{T_\tau} h(s_t)/T_\tau)$, where $\alpha \in [0, 1]$ is a tunable constant and σ is the sigmoid function. Thus, $\lambda(\tau)$ varies with the performance of the behavior policy over data.
- *Rank*: Similar to the Sigmoid labeling function, we provide a Rank labeling function $\lambda(\tau) = \alpha \sum_{\tau' \in \mathbb{D}} \mathbb{1}_{\bar{h}(\tau') \leq \bar{h}(\tau)} / n$ where n is the number of trajectories in \mathbb{D} , and $\bar{h}(\tau) = \frac{1}{T} \sum_{h_t \in \tau} h_t$.

Step 3: Relabeling r and γ Finally, we relabel the reward as \tilde{r} and the discount factor as $\tilde{\gamma}$ in each tuple of \mathbb{D} . To this end, we first convert the updated data trajectories $\{\{(s_t, a_t, r_t, h_t, \lambda_t)\}_{t=1}^{T_\tau}\}$ back into data tuples $\{(s, a, s', r, \gamma, h', \lambda')\}$, where h' and λ' denote the next-step heuristic and blending factor. Then, for each data tuple, we compute

$$\tilde{r} = r + \gamma \lambda' h' \quad \text{and} \quad \tilde{\gamma} = \gamma(1 - \lambda'), \quad (2)$$

to form a new dataset $\tilde{\mathbb{D}} := \{(s, a, s', \tilde{r}, \tilde{\gamma})\}$. Intuitively, one can interpret \tilde{r} as injecting a heuristic-dependent quantity $\gamma \lambda' h'$ into the original reward, and $\tilde{\gamma}$ as reducing bootstrapping by shrinking the original discount factor by a factor of $1 - \lambda'$. We formally explain and justify the design of \tilde{r} and $\tilde{\gamma}$ in Section 5.

5 Understanding HUBL

In this section, we take a deeper look into how HUBL works. At a high level, our theoretical analysis explains that the modification made by HUBL introduces a trade-off between bias and regret (i.e., the variance of policy learning) into the base offline RL algorithm. Our analysis provides insights as to why reshaping of rewards and discounts per (2) gives a performance boost to state-of-the-art offline RL algorithms in the experiments in Section 6.

5.1 HUBL as MDP Reshaping

We analyze HUBL by viewing it as solving a reshaped MDP $\tilde{\mathcal{M}} := (\mathcal{S}, \mathcal{A}, \mathcal{P}, \tilde{r}, \tilde{\gamma})$ constructed by blending heuristics into the original MDP. To this end, with Ω denoting the support of the data distribution, we make a simplification by assuming that both the heuristic and blending factor are functions of in- Ω states (i.e., $h(\cdot) : \Omega \rightarrow \mathbb{R}$ and $\lambda(\cdot) : \Omega \rightarrow [0, 1]$). For analysis, we them to out-of- Ω states as below:

$$h(s) = \begin{cases} h(s) & \text{for } s \in \Omega \\ 0 & \text{otherwise} \end{cases} \quad \text{and} \quad \lambda(s, s') = \begin{cases} \lambda(s') & \text{for } s, s' \in \Omega \\ 0 & \text{otherwise} \end{cases} \quad (3)$$

We note that this extension is only for the purpose of analysis, since HUBL never uses the values $h(\cdot)$ and $\lambda(\cdot)$ outside Ω ; h on out-of- Ω can have any value and the following theorems still hold.

We define the reshaped MDP $\tilde{\mathcal{M}}$ with redefined reward function and discount factor as $\tilde{r}(s, a) := r(s, a) + \gamma \mathbb{E}_{s' \sim \mathcal{P}(\cdot|s, a)} [\lambda(s, s') h(s')]$, and $\tilde{\gamma}(s, s') := \gamma(1 - \lambda(s, s'))$ respectively. Note that we

²In our implementation, we also train a value function approximator to bootstrap at the *end* of a trajectory if the trajectory ends due to timeout.

blend the original reward function with the expected heuristic and blending factor while adjusting the original discount factor correspondingly. The extent of blending is determined by the function $\lambda(\cdot)$. Notice that this reshaped MDP has a transition-dependent³ discount factor $\tilde{\gamma}(s, s')$ which is compatible with generic unifying task specification of [White, 2017]. This novel definition of transition-dependent discount factor is a key analysis technique to show that blending heuristics is effective in the *offline* setting.

Reshaped Dynamic Programming When solving this reshaped MDP by dynamic programming, the Bellman equation changes from (1) accordingly into

$$\begin{aligned} \tilde{Q}^\pi(s, a) &= \tilde{r}(s, a) + \mathbb{E}_{s' \sim \mathcal{P}(\cdot|s, a)}[\tilde{\gamma}(s, s')\tilde{V}^\pi(s')] \\ &= r(s, a) + \underbrace{\gamma \mathbb{E}_{s' \sim \mathcal{P}(\cdot|s, a)}[(1 - \lambda(s, s'))\tilde{V}^\pi(s')]}_{\text{bootstrapping}} + \underbrace{\gamma \mathbb{E}_{s' \sim \mathcal{P}(\cdot|s, a)}[\lambda(s, s')h(s')]}_{\text{heuristic}}. \end{aligned} \quad (4)$$

Here \tilde{Q}^π denotes the Q -function of policy π in $\tilde{\mathcal{M}}$, and \tilde{V}^π denotes π 's value function. Compared to the original Bellman equation (1), it can be seen that $\lambda(\cdot)$ blends the heuristic with bootstrapping: the bigger λ 's values, the more bootstrapping is replaced by the heuristic. The effect of solving HUBL's reshaped MDP $\tilde{\mathcal{M}}$ is twofold. On the one hand, $\tilde{\mathcal{M}}$ is different from the original MDP \mathcal{M} : the optimal policy for $\tilde{\mathcal{M}}$ may not be optimal for \mathcal{M} , so solving for $\tilde{\mathcal{M}}$ could potentially lead to performance bias. On the other hand, $\tilde{\mathcal{M}}$ has a smaller discount factor and thus is easier to solve than \mathcal{M} , as the agent needs to plan for a smaller horizon. Therefore, we can think of applying HUBL to offline RL problems as performing a bias-variance trade-off, which reduces the learning variance due to bootstrapping at the cost of the bias due to using a suboptimal heuristic. We will explain this more concretely next.

5.2 Bias-Regret Decomposition

The insight that HUBL reshapes the Bellman equation that the offline RL algorithm uses allows us to characterize HUBL's effects on policy learning. Namely, we use the modified Bellman equation from (4) to decompose the performance of the learned policy into bias and regret terms.

Theorem 1. *For any $h : \Omega \rightarrow \mathbb{R}$, $\lambda : \Omega \rightarrow [0, 1]$, and policy π , with V^* as the value function of the optimal policy, it holds that $V^*(d_0) - V^\pi(d_0) = \text{Bias}(\pi, h, \lambda) + \text{Regret}(\pi, h, \lambda)$, where*

$$\begin{aligned} \text{Bias}(\pi, h, \lambda) &:= \frac{\gamma}{1 - \gamma} \mathbb{E}_{(s, a, s') \sim d^{\pi^*}}[\lambda(s')(\tilde{V}^{\pi^*}(s') - h(s')) | s, s' \in \Omega] \\ \text{Regret}(\pi, h, \lambda) &:= \tilde{V}^{\pi^*}(d_0) - \tilde{V}^\pi(d_0) + \frac{\gamma}{1 - \gamma} \mathbb{E}_{(s, a, s') \sim d^\pi}[\lambda(s')(h(s') - \tilde{V}^\pi(s')) | s, s' \in \Omega]. \end{aligned}$$

The performance of π depends on both bias and regret. The bias term describes the discrepancy caused by solving the reshaped MDP with $\lambda(\cdot)$. When $\lambda(s') = 0$, the bias becomes zero. The regret term describes the performance of the learned policy in the reshaped MDP. Intuitively, at states whose successors have bigger $\lambda(s')$ values, the reshaped MDP has a smaller discount factor and thus is easier to solve, which leads to smaller regret (i.e., smaller values for $\tilde{V}^{\pi^*}(d_0) - \tilde{V}^\pi(d_0)$). Therefore, solving a HUBL-reshaped MDP induces a bias term but may generate a smaller regret.

Remark The critical difference – and novelty – of Theorem 1 compared to existing theoretical results for RL with heuristics in the offline setting is that both the bias and regret in Theorem 1 depend only on states *in the data distribution support* Ω . This is crucial, because in the offline setting we have no access to observations beyond Ω . In contrast, if in the preceding analysis we replace Theorem 1 by, for example, Lemma A.1 from Cheng et al. [2021] with a constant λ , we will get a performance decomposition $V^*(d_0) - V^\pi(d_0) = (V^*(d_0) - \tilde{V}^*(d_0)) + \frac{\gamma\lambda}{1-\gamma} \mathbb{E}_{s, a \sim d^\pi} \mathbb{E}_{s' | s, a}[h(s') - \tilde{V}^*(s')] + (1 - \lambda)(\tilde{V}^*(d_0) - \tilde{V}^\pi(d_0)) + \frac{\lambda}{1-\gamma}(\tilde{V}^*(d^\pi) - \tilde{V}^\pi(d^\pi))$. The decomposition, however, suggests that the out-of- Ω values of $\lambda(s)$ or $h(s)$ are important to the performance of HUBL.

5.3 Finite Sample Analysis for Bias and Regret

The finite-sample analysis of policy learning that we provide next illustrates more concretely how HUBL trades off bias and regret. Our analysis uses offline value iteration with lower confidence

³A special case of trajectory-dependent discounts.

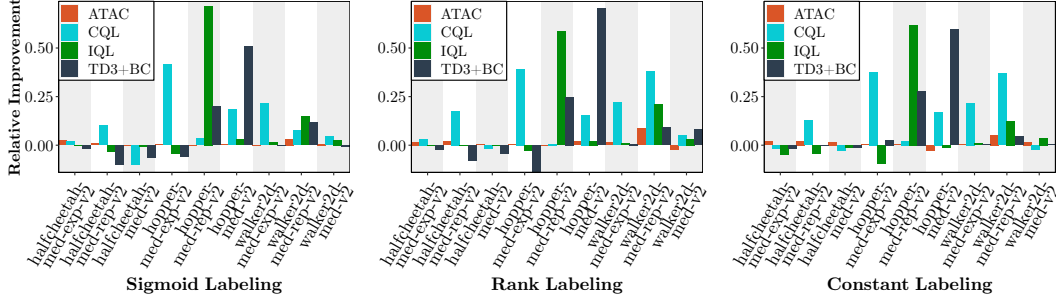


Figure 2: Relative improvement of HUBL on 9 D4RL datasets.

bound (VI-LCB) [Rashidinejad et al., 2021] as the base offline RL method. Following its original convention, we make some technical simplifications to make the presentation cleaner. Specifically, we consider a tabular setting with $\lambda(s) = \alpha \in [0, 1]$ for $s \in \Omega$ as a constant value, which can be interpreted as the quality of the behavior policy averaged across states. Note that despite $\lambda(s) = \alpha$ is a constant on Ω , the reshaped MDP is still defined by $\lambda(s, s')$ in (3) (i.e., $\lambda(s, s') = \alpha$ if $s, s' \in \Omega$ and zero otherwise). We postpone the detailed procedure of VI-LCB with HUBL in Appendix C due to space limitation.

Theorem 2 summarizes our finite-sample results. The proof of Theorem 2 can be found in Appendix B.

Theorem 2. *Under the setup described above, assume that the heuristic $h(\cdot)$ satisfies $h(s) = V^\mu(s)$ for any $s \in \Omega$. Then the bias and the regret in Theorem 1 are bounded by*

$$\text{Bias}(\hat{\pi}, \lambda) \leq \frac{\gamma\lambda}{1-\gamma} \mathbb{E}_{(s,a,s') \sim d^{\pi^*}} [V^*(s') - V^\mu(s') | s, s' \in \Omega],$$

$$\mathbb{E}_{\mathbb{D}} [\text{Regret}(\hat{\pi}, \lambda)] \lesssim \min \left(V_{max}, \sqrt{\frac{V_{max}^2(1-\gamma)|S|}{N(1-\gamma(1-\lambda))^4}} \left(\sqrt{\max_{s,a} \frac{d^{\pi^*}(s,a)}{\mu(s,a)}} + \frac{\gamma\lambda}{1-\gamma} \sqrt{\max_{(s,a) \in \Omega} \frac{1}{\mu(s,a)}} \right) \right)$$

where V_{max} denotes a constant upper bound for the value function.

For the bias bound, the assumption $h(s) = V^\mu(s)$ for any $s \in \Omega$ is made for the ease of presentation. If it does not hold, an additive error term can be introduced in the bias bound to capture that. For the regret bound, $\max_{s,a} \frac{d^{\pi^*}(s,a;d_0)}{\mu(s,a)}$ can be infinite, whereby the best regret bound is just V_{max} . But when it is bounded as assumed by existing works [Rashidinejad et al., 2021], our results demonstrate how N , γ and λ affect the regret bound.

The implications of Theorem 2 are threefold. First of all, it provides a finite-sample performance guarantee for HUBL with VI-LCB under the tabular setting. Compared with the performance bound of the original VI-LCB, $\min \left(V_{max}, \sqrt{\frac{V_{max}^2|S|}{(1-\gamma)^3N}} \max_{s,a} \frac{d^{\pi^*}(s,a)}{\mu(s,a)} \right)$, HUBL shrinks the discount factor by $1 - \lambda$ and thus potentially improves the performance while inducing bias. Second, Theorem 2 hints at the source of HUBL’s bias and regret of HUBL. The bias is related to the the performance of the behavior (data-collection) policy, characterized by $V^*(s) - V^\mu(s)$. In the extreme case of data being collected by an expert policy, the bias induced by HUBL is 0. The regret is affected by $\frac{d^{\pi^*}(s,a)}{\mu(s,a)}$, which describes the deviation of the optimal policy from the data distribution. Finally, Theorem 2 also provides guidance on how to construct a blending factor function $\lambda(\cdot)$. To reduce bias, $\lambda(s)$ should be small at states where $V^*(s) - V^\mu(s)$ is small. To reduce regret, $\lambda(\cdot)$ should be generally large but small at states where the learned policy is likely to deviate from the behavior policy. Therefore, an ideal $\lambda(\cdot)$ should be large when the behavior policy is close to optimal but small when it deviates from the optimal policy. This is consistent with our design principle in Section 4.2.

6 Experiments

We study 27 benchmark datasets in D4RL and Meta-World. We show that HUBL is able to improve the performance of existing offline RL methods by 9% with easy modifications and simple hyperparameter tuning. Remarkably, in some datasets where the base offline RL shows inconsistent performance and especially underperforms, HUBL can achieve more than 50% performance improvement.

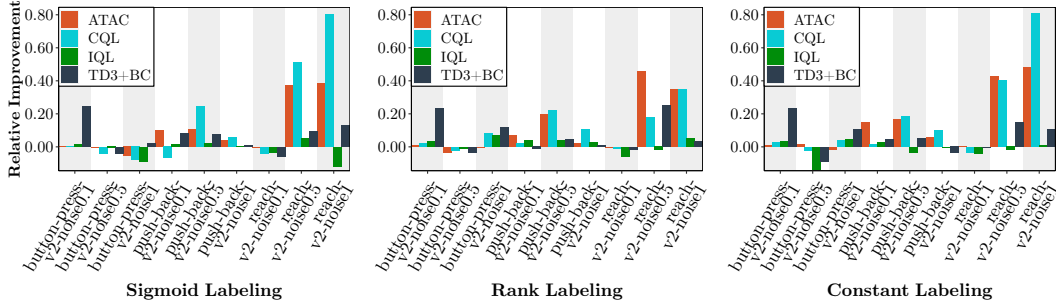


Figure 3: Relative improvement of HUBL on Meta-World datasets (Part I).

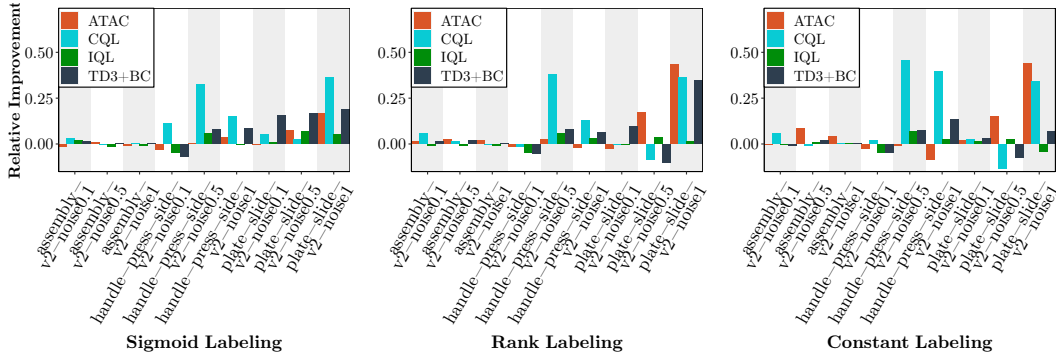


Figure 4: Relative improvement of HUBL on Meta-World datasets (Part II).

HUBL variants and base offline RL methods We implement HUBL with four state-of-the-art offline RL algorithms as base methods: CQL [Kumar et al., 2020], TD3+BC [Fujimoto and Gu, 2021], IQL [Kostrikov et al., 2022], and ATAC [Cheng et al., 2022]. For each base method, we compare the performance of its original version to its performance with HUBL running three different blending strategies discussed in Section 4.2: Constant, Sigmoid and Rank. Thus, we experiment with 16 different methods in total. The implementation details of the base methods are in Appendix D.1.

Metrics We use relative normalized score improvement, abbreviated as *relative improvement*, as a measure of HUBL’s performance improvement. Specifically, for a given task and base method, we first compute the normalized score r_{base} achieved by the base method, and then the normalized score r_{HUBL} of HUBL. The relative normalized score improvement is defined as $\frac{r_{HUBL} - r_{base}}{|r_{base}|}$. We report the relative improvement of HUBL averaged over three seeds $\{0, 1, 10\}$ in this section, with *standard deviations*, *base method performance*, *behavior cloning performance* and *absolute normalized scores* provided in Appendix D.2, D.5, and D.6.

Hyperparameter Tuning For each dataset, the hyperparameters of the base methods are tuned over six different configurations suggested by the original papers. HUBL has one extra hyperparameter, α , which is *fixed* for all the datasets but different for each base method. Specifically, α is selected from $\{0.001, 0.01, 0.1\}$ according to the relative improvement averaged over all the datasets. In practice, we notice that a single choice of α around 0.1 is sufficient for good performance across most base offline RL methods and datasets as demonstrated by the sensitivity analysis in Appendix D.3.

6.1 D4RL Experiments

Results We study 9 benchmark datasets in D4RL. The relative improvement due to HUBL is reported in Figure 2. First, despite being simple and needing little hyperparameter tuning, HUBL improves the performance of base methods in most settings and only slightly hurts in some expert datasets where base offline RL methods are already performing very well with little space of improvement. Second, there are cases where HUBL achieve very significant relative improvement—more than 50%. Such big improvement happens in the datasets where the base method shows inconsistent performance and underperforms other offline RL algorithms. HUBL solves this inconsistent performance issue by simply relabeling the data. Further, HUBL improves performance even on data with few expert trajec-

ories like hopper-med-rep-v2, walker2d-med-rep-v2, and hopper-med-v2, because HUBL conducts more bootstrapping and relies less on the heuristic on suboptimal trajectories (see Section 4.2).

Ablation Studies Note that HUBL relabels both the reward and the discount factor, per (2). However, existing methods like Hu et al. [2022] suggest that a lower discount factor *alone* without blending heuristics into rewards can in general improve offline RL. Therefore, to demonstrate the necessity of modifying both the discount factor and rewards like (2), we consider ablation methods which only shrink the discount factor as $\tilde{\gamma}$ without \tilde{r} . The achieved average relative improvement of these ablations is reported and compared with that of HUBL in Table 1. HUBL consistently outperforms these ablations, which justifies HUBL’s coordinated modifications in both the reward and the discount factor. The advantage of HUBL is also consistent with our theoretical analysis predicts. The considered ablations do not modify the rewards and thus are equivalent to solving $\tilde{Q}^\pi(s, a) = r(s, a) + \gamma \mathbb{E}_{s' \sim \mathcal{P}(\cdot|s, a)}[(1 - \lambda(s'))\tilde{V}^\pi(s')]$. Comparing it with (1), the solution will be consistently smaller than the true Q -function, inducing a pessimistic bias. Crucially, this bias is much more challenging to tackle than the bias induced by HUBL, because the former is inevitable even when the data is collected by an expert policy.

Table 1: Average relative improvement of ablations without \tilde{r} .

ATAC	Sigmoid	Rank	Constant
Ablations without \tilde{r}	-0.01	-0.02	-0.02
HUBL	0.01	0.02	0.01
CQL	Sigmoid	Rank	Constant
Ablations without \tilde{r}	0.04	0.04	0.04
HUBL	0.11	0.16	0.13
IQL	Sigmoid	Rank	Constant
Ablations without \tilde{r}	-0.04	-0.04	-0.07
HUBL	0.09	0.09	0.06
TD3+BC	Sigmoid	Rank	Constant
Ablations without \tilde{r}	-0.01	-0.03	-0.04
HUBL	0.06	0.09	0.1

6.2 Meta-World Experiments

We also run considered methods on tasks from the Meta-World benchmark. We study 18 datasets collected following the procedure detailed in Appendix D.4. These problems are goal-oriented, which is in contrast to locomotion tasks in the previous D4RL experiments. The achieved relative improvement of HUBL in the Meta-World experiments are reported in Figure 3 and Figure 4. HUBL is again able to generally improve the performance of existing offline RL methods.

6.3 Comparisons among blending strategies

We present results for three different blending factor designs for HUBL (constant, sigmoid, and rank), where the rank blending outperforms the other two. With 27 datasets and 4 base methods, we have 108 cases covered by Figure 2 3 and 4 We count the number of cases where a given blending strategy provides the best performance among the three, and the results are reported in Table 2. We can see that Rank is favored on average.

	Sigmoid	Rank	Constant
Wins	30	46	32

Table 2: Comparison among blending strategies

7 Conclusion

In this work, we propose HUBL, a method for improving the performance offline RL methods by blending heuristics with bootstrapping. HUBL is easy to implement and is generally applicable to various of offline RL methods. Empirically, we demonstrate the performance improvement of HUBL on 27 datasets in D4RL and Meta-World. We also provide a theoretic finite-sample performance bound for HUBL, which also sheds lights on HUBL’s bias-regret trade-off and blending factor designs. To our knowledge, our theoretical analysis is the first formal proof to show the effectiveness of using heuristics in the offline setting.

Limitations and Future Work In our current framework, HUBL calculate heuristics by Monte-Carlo returns. While this is a feasible and effective strategy in common practical scenarios where data are collected as trajectories, we remark that this strategy is not applicable to batch datasets with only very short trajectories or even no trajectories (i.e., data of just disconnected transition tuples). For such scenarios, HUBL requires other heuristic calculation strategies. We consider this direction as our future work. We also plan to apply HUBL to other tasks in healthcare and finance [Alaluf et al., 2022, Geng et al., 2019, 2018] where collecting data is especially expensive.

References

- Melda Alaluf, Giulia Crippa, Sinong Geng, Zijian Jing, Nikhil Krishnan, Sanjeev Kulkarni, Wyatt Navarro, Ronnie Sircar, and Jonathan Tang. Reinforcement learning paycheck optimization for multivariate financial goals. *Risk & Decision Analysis*, 2022.
- Wissam Bejjani, Rafael Papallas, Matteo Leonetti, and Mehmet R Dogar. Planning with a receding horizon for manipulation in clutter using a learned value function. In *2018 IEEE-RAS 18th International Conference on Humanoid Robots (Humanoids)*, pages 1–9. IEEE, 2018.
- Marc Bellemare, Sriram Srinivasan, Georg Ostrovski, Tom Schaul, David Saxton, and Remi Munos. Unifying count-based exploration and intrinsic motivation. *Advances in neural information processing systems*, 29, 2016.
- David Blackwell. Discrete dynamic programming. *The Annals of Mathematical Statistics*, pages 719–726, 1962.
- Ching-An Cheng, Andrey Kolobov, and Adith Swaminathan. Heuristic-guided reinforcement learning. *Advances in Neural Information Processing Systems*, 34:13550–13563, 2021.
- Ching-An Cheng, Tengyang Xie, Nan Jiang, and Alekh Agarwal. Adversarially trained actor critic for offline reinforcement learning. *arXiv preprint arXiv:2202.02446*, 2022.
- Gabriel Dulac-Arnold, Nir Levine, Daniel J Mankowitz, Jerry Li, Cosmin Paduraru, Sven Gowal, and Todd Hester. Challenges of real-world reinforcement learning: definitions, benchmarks and analysis. *Machine Learning*, 110(9):2419–2468, 2021.
- Justin Fu, Katie Luo, and Sergey Levine. Learning robust rewards with adversarial inverse reinforcement learning. *arXiv preprint arXiv:1710.11248*, 2017.
- Justin Fu, Aviral Kumar, Ofir Nachum, George Tucker, and Sergey Levine. D4rl: Datasets for deep data-driven reinforcement learning, 2020.
- Scott Fujimoto and Shixiang Shane Gu. A minimalist approach to offline reinforcement learning. *Advances in neural information processing systems*, 34:20132–20145, 2021.
- Scott Fujimoto, David Meger, and Doina Precup. Off-policy deep reinforcement learning without exploration. In *International conference on machine learning*, pages 2052–2062. PMLR, 2019.
- S Geng, Z Kuang, PL Peissig, D Page, L Maursetter, and KE Hansen. Parathyroid hormone independently predicts fracture, vascular events, and death in patients with stage 3 and 4 chronic kidney disease. *Osteoporosis International*, 30:2019–2025, 2019.
- Sinong Geng, Zhaobin Kuang, Peggy Peissig, and David Page. Temporal poisson square root graphical models. *Proceedings of machine learning research*, 80:1714, 2018.
- Sinong Geng, Houssam Nassif, Carlos Manzanares, Max Reppen, and Ronnie Sircar. Deep pqr: Solving inverse reinforcement learning using anchor actions. In *International Conference on Machine Learning*, pages 3431–3441. PMLR, 2020.
- Sinong Geng, Houssam Nassif, and Carlos A Manzanares. A data-driven state aggregation approach for dynamic discrete choice models. *arXiv preprint arXiv:2304.04916*, 2023.
- Caglar Gulcehre, Ziyu Wang, Alexander Novikov, Thomas Paine, Sergio Gómez, Konrad Zolna, Rishabh Agarwal, Josh S Merel, Daniel J Mankowitz, Cosmin Paduraru, et al. RL unplugged: A suite of benchmarks for offline reinforcement learning. *Advances in Neural Information Processing Systems*, 33:7248–7259, 2020.
- David Hoeller, Farbod Farshidian, and Marco Hutter. Deep value model predictive control. In *Conference on Robot Learning*, pages 990–1004. PMLR, 2020.
- Hao Hu, Yiqin Yang, Qianchuan Zhao, and Chongjie Zhang. On the role of discount factor in offline reinforcement learning. In *International Conference on Machine Learning*, pages 9072–9098. PMLR, 2022.

- Ehsan Imani, Eric Graves, and Martha White. An off-policy policy gradient theorem using emphatic weightings. *Advances in Neural Information Processing Systems*, 31, 2018.
- Nan Jiang, Alex Kulesza, Satinder Singh, and Richard Lewis. The dependence of effective planning horizon on model accuracy. In *Proceedings of the 2015 International Conference on Autonomous Agents and Multiagent Systems*, pages 1181–1189, 2015.
- Ray Jiang, Tom Zahavy, Zhongwen Xu, Adam White, Matteo Hessel, Charles Blundell, and Hado Van Hasselt. Emphatic algorithms for deep reinforcement learning. In *International Conference on Machine Learning*, pages 5023–5033. PMLR, 2021.
- Ying Jin, Zhuoran Yang, and Zhaoran Wang. Is pessimism provably efficient for offline rl? In *International Conference on Machine Learning*, pages 5084–5096. PMLR, 2021.
- Diederik P Kingma and Jimmy Ba. Adam: A method for stochastic optimization. *arXiv preprint arXiv:1412.6980*, 2014.
- Ilya Kostrikov, Ashvin Nair, and Sergey Levine. Offline reinforcement learning with implicit Q-learning. In *ICLR*, 2022.
- Aviral Kumar, Justin Fu, Matthew Soh, George Tucker, and Sergey Levine. Stabilizing off-policy q-learning via bootstrapping error reduction. *Advances in Neural Information Processing Systems*, 32, 2019.
- Aviral Kumar, Aurick Zhou, George Tucker, and Sergey Levine. Conservative q-learning for offline reinforcement learning. *Advances in Neural Information Processing Systems*, 33:1179–1191, 2020.
- Sascha Lange, Thomas Gabel, and Martin Riedmiller. Batch reinforcement learning. In *Reinforcement learning*, pages 45–73. Springer, 2012.
- Georg Ostrovski, Marc G Bellemare, Aäron Oord, and Rémi Munos. Count-based exploration with neural density models. In *International conference on machine learning*, pages 2721–2730. PMLR, 2017.
- Marek Petrik and Bruno Scherrer. Biasing approximate dynamic programming with a lower discount factor. *Advances in neural information processing systems*, 21, 2008.
- Paria Rashidinejad, Banghua Zhu, Cong Ma, Jiantao Jiao, and Stuart Russell. Bridging offline reinforcement learning and imitation learning: A tale of pessimism. *Advances in Neural Information Processing Systems*, 34:11702–11716, 2021.
- Harm Seijen and Rich Sutton. True online td (λ). In *International Conference on Machine Learning*, pages 692–700. PMLR, 2014.
- Richard S Sutton and Andrew G Barto. *Reinforcement learning: An introduction*. MIT press, 2018.
- Richard S Sutton, A Rupam Mahmood, and Martha White. An emphatic approach to the problem of off-policy temporal-difference learning. *The Journal of Machine Learning Research*, 17(1): 2603–2631, 2016.
- Harm Van Seijen, Mehdi Fatemi, and Arash Tavakoli. Using a logarithmic mapping to enable lower discount factors in reinforcement learning. *Advances in Neural Information Processing Systems*, 32, 2019.
- Martha White. Unifying task specification in reinforcement learning. In *International Conference on Machine Learning*, pages 3742–3750. PMLR, 2017.
- Albert Wilcox, Ashwin Balakrishna, Jules Dedieu, Wyame Benslimane, Daniel Brown, and Ken Goldberg. Monte carlo augmented actor-critic for sparse reward deep reinforcement learning from suboptimal demonstrations. *arXiv preprint arXiv:2210.07432*, 2022.
- Robert Wright, Steven Loscalzo, Philip Dexter, and Lei Yu. Exploiting multi-step sample trajectories for approximate value iteration. In *Machine Learning and Knowledge Discovery in Databases: European Conference, ECML PKDD 2013, Prague, Czech Republic, September 23-27, 2013, Proceedings, Part I 13*, pages 113–128. Springer, 2013.

- Tianhe Yu, Deirdre Quillen, Zhanpeng He, Ryan Julian, Karol Hausman, Chelsea Finn, and Sergey Levine. Meta-world: A benchmark and evaluation for multi-task and meta reinforcement learning. In *Conference on robot learning*, pages 1094–1100. PMLR, 2020.
- Andrea Zanette, Ching-An Cheng, and Alekh Agarwal. Cautiously optimistic policy optimization and exploration with linear function approximation. In *Conference on Learning Theory*, pages 4473–4525. PMLR, 2021.
- Mingyuan Zhong, Mikala Johnson, Yuval Tassa, Tom Erez, and Emanuel Todorov. Value function approximation and model predictive control. In *2013 IEEE symposium on adaptive dynamic programming and reinforcement learning (ADPRL)*, pages 100–107. IEEE, 2013.

A Extended Results of Theorem 1

Below we prove the statement which is a restatement of theorem 1.

Theorem 3. For any $\lambda : \Omega \rightarrow [0, 1]$ and any $h : \Omega \rightarrow \mathbb{R}$, it holds

$$\begin{aligned} V^*(s_0) - V^{\hat{\pi}}(s_0) &= \left(\tilde{V}^{\pi^*}(s_0) - \tilde{V}^{\hat{\pi}}(s_0) \right) \\ &\quad + \frac{\gamma}{1-\gamma} \mathbb{E}_{(s,a,s') \sim d^{\pi^*}} [\lambda(s')(\tilde{V}^{\pi^*}(s') - h(s')) | s, s' \in \Omega] \\ &\quad + \frac{\gamma}{1-\gamma} \mathbb{E}_{(s,a,s') \sim d^{\pi}} [\lambda(s')(h(s') - \tilde{V}^{\hat{\pi}}(s')) | s, s' \in \Omega] \end{aligned} \quad (5)$$

A.1 Technical Lemmas

Lemma 4. For any policy π ,

$$V^\pi(s_0) - \tilde{V}^\pi(s_0) = \frac{\gamma}{1-\gamma} \mathbb{E}_{(s,a,s') \sim d^\pi} [\lambda(s')(\tilde{V}^\pi(s') - h(s')) | s, s' \in \Omega].$$

Proof. By the definition of $\lambda(s, s')$:

$$\begin{aligned} V^\pi(s_0) - \tilde{V}^\pi(s_0) &= \frac{1}{1-\gamma} \mathbb{E}_{(s,a,s') \sim d^\pi} [r(s, a) + \gamma \tilde{V}^\pi(s') - \tilde{V}^\pi(s)] \\ &= \frac{1}{1-\gamma} \mathbb{E}_{(s,a,s') \sim d^\pi} [r(s, a) + \gamma \tilde{V}^\pi(s') - r(s, a) - \gamma \lambda(s, s') h(s') + \gamma(1 - \lambda(s, s')) \tilde{V}^\pi(s')] \\ &= \frac{\gamma}{1-\gamma} \mathbb{E}_{(s,a,s') \sim d^\pi} [\lambda(s, s')(\tilde{V}^\pi(s') - h(s'))] \\ &= \frac{\gamma}{1-\gamma} \mathbb{E}_{(s,a,s') \sim d^\pi} [\lambda(s, s')(\tilde{V}^\pi(s') - h(s')) | s, s' \in \Omega] \\ &= \frac{\gamma}{1-\gamma} \mathbb{E}_{(s,a,s') \sim d^\pi} [\lambda(s')(\tilde{V}^\pi(s') - h(s')) | s, s' \in \Omega] \end{aligned}$$

□

A.2 Proof of Theorem 3

To prove the theorem, we decompose the regret into the following terms:

$$V^*(s_0) - V^{\hat{\pi}}(s_0) = \left(V^*(s_0) - \tilde{V}^{\pi^*}(s_0) \right) + \left(\tilde{V}^{\pi^*}(s_0) - \tilde{V}^{\hat{\pi}}(s_0) \right) + \left(\tilde{V}^{\hat{\pi}}(s_0) - V^{\hat{\pi}}(s_0) \right)$$

We apply theorem 4 to rewrite the first and the last terms as

$$\begin{aligned} V^*(s_0) - \tilde{V}^{\pi^*}(s_0) &= \frac{\gamma}{1-\gamma} \mathbb{E}_{(s,a,s') \sim d^{\pi^*}} [\lambda(s')(\tilde{V}^{\pi^*}(s') - h(s')) | s, s' \in \Omega] \\ \tilde{V}^{\hat{\pi}}(s_0) - V^{\hat{\pi}}(s_0) &= \frac{\gamma}{1-\gamma} \mathbb{E}_{(s,a,s') \sim d^\pi} [\lambda(s')(h(s') - \tilde{V}^{\hat{\pi}}(s')) | s, s' \in \Omega]. \end{aligned}$$

Combining the two completes the proof.

B Extended Results for Theorem 2

B.1 Technical Lemmas

Lemma 5. Under the setup of Theorem 2, $\tilde{V}^\mu(s) = V^\mu(s)$.

Proof. Since Ω is the support of μ , this can be shown by the following: for $s \in \Omega$,

$$\begin{aligned}
& \tilde{V}^\mu(s) - V^\mu(s) \\
&= \mathbb{E}_{a \sim \mu|s} \mathbb{E}_{s'|s,a} [r(s,a) + \gamma \lambda(s,s') h(s') + \gamma(1 - \lambda(s,s')) \tilde{V}^\mu(s') - r(s,a) - \gamma V^\mu(s')] \\
&= \mathbb{E}_{a \sim \mu|s} \mathbb{E}_{s'|s,a} [r(s,a) + \gamma \lambda(s,s') h(s') + \gamma(1 - \lambda(s,s')) \tilde{V}^\mu(s') - r(s,a) - \gamma V^\mu(s') | s' \in \Omega] \\
&= \mathbb{E}_{a \sim \mu|s} \mathbb{E}_{s'|s,a} [r(s,a) + \gamma \lambda(s,s') V^\mu(s') + \gamma(1 - \lambda(s,s')) \tilde{V}^\mu(s') - r(s,a) - \gamma V^\mu(s') | s' \in \Omega] \\
&= \gamma \mathbb{E}_{a \sim \mu|s} \mathbb{E}_{s'|s,a} [(1 - \lambda(s,s')) (\tilde{V}^\mu(s') - V^\mu(s')) | s' \in \Omega].
\end{aligned}$$

Since $\gamma < 1$, then by an argument of contraction, we have $\tilde{V}^\mu(s) - V^\mu(s) = 0$ for $s \in \Omega$. □

Lemma 6. Assume $h(s) \leq V^*(s)$, $\forall s \in \mathcal{S}$. It holds that $\tilde{V}^{\pi^*}(s) \leq V^*(s)$ for all $s \in \mathcal{S}$.

Proof.

$$\begin{aligned}
\tilde{V}^{\pi^*}(s) &= r(s,a) + \gamma \mathbb{E}_{s'|s,a} [\lambda(s,s') h(s') + (1 - \lambda(s,s')) \tilde{V}^{\pi^*}(s')] \\
&= V^*(s) + \gamma \mathbb{E}_{s'|s,a} [\lambda(s,s') h(s') + (1 - \lambda(s,s')) \tilde{V}^{\pi^*}(s') - V^*(s')] \\
&= V^*(s) + \gamma \mathbb{E}_{s'|s,a} [\lambda(s,s') (h(s') - V^*(s')) + (1 - \lambda(s,s')) (\tilde{V}^{\pi^*}(s') - V^*(s'))] \\
&\leq V^*(s) + \gamma \mathbb{E}_{s'|s,a} [(1 - \lambda(s,s')) (\tilde{V}^{\pi^*}(s') - V^*(s'))]
\end{aligned}$$

where in the inequality we used $h(s) \leq V^*(s)$. Then by a contraction argument, we can then show $\tilde{V}^{\pi^*}(s) - V^{\pi^*}(s) \leq 0$ □

Lemma 7 (Bias Upperbound). Under the assumptions of Theorem 2, the bias component can be bounded by:

$$\text{Bias}(\hat{\pi}, \lambda) \leq \frac{\lambda\gamma}{1-\gamma} \mathbb{E}_{(s,a,s') \sim d^{\pi^*}} [V^*(s') - V^\mu(s') | s, s' \in \Omega].$$

Proof. Review the bias component

$$\text{Bias}(\hat{\pi}, \lambda) := \frac{\gamma}{1-\gamma} \mathbb{E}_{(s,a,s') \sim d^{\pi^*}} [\lambda(s') (\tilde{V}^{\pi^*}(s') - h(s')) | s, s' \in \Omega].$$

Under the assumptions of Theorem 2, we derive

$$\text{Bias}(\hat{\pi}, \lambda) = \frac{\lambda\gamma}{1-\gamma} \mathbb{E}_{(s,a,s') \sim d^{\pi^*}} [\tilde{V}^{\pi^*}(s') - V^*(s') + V^*(s') - V^\mu(s') | s, s' \in \Omega].$$

Next by Lemma 6 we have $\frac{\lambda\gamma}{1-\gamma} \mathbb{E}_{(s,a,s') \sim d^{\pi^*}} [\tilde{V}^{\pi^*}(s') - V^*(s') | s, s' \in \Omega] \leq 0$, and thus

$$\text{Bias}(\hat{\pi}, \lambda) \leq \frac{\lambda\gamma}{1-\gamma} \mathbb{E}_{(s,a,s') \sim d^{\pi^*}} [V^*(s') - V^\mu(s') | s, s' \in \Omega].$$

□

Lemma 8. The difference between $V^*(s)$ and $\tilde{V}^{\pi^*}(s)$ can be derived as

$$V^*(s) - \tilde{V}^{\pi^*}(s) = \mathbb{E}_{\rho^{\pi^*}(s)} \left[\sum_{t=1}^{\infty} [\lambda(1-\lambda)^{t-1} \gamma^t (V^*(s_t) - h(s_t))] \right].$$

Proof. By the dynamic programming equation in both the original and shaped MDP.

$$\begin{aligned}
V^*(s) - \tilde{V}^{\pi^*}(s) &= \gamma(1-\lambda) \mathbb{E}_{a \sim \pi^*(\cdot; s)} [\mathbb{E}_{s'|s,a} [V^*(s') - \tilde{V}^{\pi^*}(s')]] \\
&\quad + \gamma \lambda \mathbb{E}_{a \sim \pi^*(\cdot; s)} [\mathbb{E}_{s'|s,a} [V^*(s') - h(s')]].
\end{aligned} \tag{6}$$

Then, we use (6) recursively:

$$V^*(s) - \tilde{V}^{\pi^*}(s) = \lambda \mathbb{E}_{\rho^{\pi^*}(s)} \left[\sum_{t=1}^{\infty} [(1-\lambda)^{t-1} \gamma^t (V^*(s_t) - h(s_t))] \right].$$

□

Lemma 9 (Regret Upperbound). *The expected regret is bounded by*

$$\begin{aligned} \mathbb{E}_{\mathbb{D}}[\text{Regret}(\hat{\pi}, \lambda(\cdot))] &\lesssim \min \left(V_{max}, V_{max} \sqrt{\frac{(1-\gamma)|\mathcal{S}| \max_{s,a} \frac{d^{\pi^*}(s,a;d_0)}{\mu(s,a)}}{N(1-\gamma(1-\lambda))^4}} \right) \\ &\quad + \frac{\gamma\lambda}{1-\gamma} \min \left(V_{max}, V_{max} \sqrt{\frac{(1-\gamma)|\mathcal{S}| \frac{1}{\min_{(s,a) \in \Omega} \mu(s,a)}}{N(1-\gamma(1-\lambda))^4}} \right). \end{aligned}$$

Proof. Under the setups in Theorem 2, we have

$$\text{Regret}(\hat{\pi}, \lambda(\cdot)) = \tilde{V}^{\pi^*}(d_0) - \tilde{V}^{\hat{\pi}}(d_0) + \frac{\gamma\lambda}{1-\gamma} \mathbb{E}_{(s,a,s') \sim d^{\hat{\pi}}} [V^\mu(s') - \tilde{V}^{\hat{\pi}}(s') | s, s' \in \Omega].$$

Further by Lemma 5, we can replace V^μ by \tilde{V}^μ :

$$\text{Regret}(\hat{\pi}, \lambda(\cdot)) = \tilde{V}^{\pi^*}(d_0) - \tilde{V}^{\hat{\pi}}(d_0) + \frac{\gamma\lambda}{1-\gamma} \mathbb{E}_{(s,a,s') \sim d^{\hat{\pi}}} [\tilde{V}^\mu(s') - \tilde{V}^{\hat{\pi}}(s') | s, s' \in \Omega]. \quad (7)$$

Then, by Lemma 10,

$$\mathbb{E}_{\mathbb{D}}[\tilde{V}^{\pi^*}(d_0) - \tilde{V}^{\hat{\pi}}(d_0)] \lesssim \min \left(V_{max}, V_{max} \sqrt{\frac{(1-\gamma)|\mathcal{S}| \max_{s,a} \frac{d^{\pi^*}(s,a;d_0)}{\mu(s,a)}}{N(1-\gamma(1-\lambda))^4}} \right), \quad (8)$$

and

$$\mathbb{E}_{\mathbb{D}}[\tilde{V}^\mu(d^{\hat{\pi}}) - \tilde{V}^{\hat{\pi}}(d^{\hat{\pi}})] \lesssim \min \left(V_{max}, V_{max} \sqrt{\frac{(1-\gamma)|\mathcal{S}| \max_{s,a} \frac{d^\mu(s,a;d^{\hat{\pi}})}{\mu(s,a)}}{N(1-\gamma(1-\lambda))^4}} \right).$$

Note that, by Lemma 11, $d^{\hat{\pi}}$ stays in Ω . Therefore, we get $\max_{s,a} \frac{d^\mu(s,a;d^{\hat{\pi}})}{\mu(s,a)} = \max_{s,a \in \Omega} \frac{d^\mu(s,a;d^{\hat{\pi}})}{\mu(s,a)} \leq \frac{1}{\min_{(s,a) \in \Omega} \mu(s,a)}$, which leads to

$$\mathbb{E}_{\mathbb{D}}[\tilde{V}^\mu(d^{\hat{\pi}}) - \tilde{V}^{\hat{\pi}}(d^{\hat{\pi}})] \lesssim \min \left(V_{max}, V_{max} \sqrt{\frac{(1-\gamma)|\mathcal{S}| \frac{1}{\min_{(s,a) \in \Omega} \mu(s,a)}}{N(1-\gamma(1-\lambda))^4}} \right). \quad (9)$$

Take (8) and (9) into (7), we derive

$$\begin{aligned} \mathbb{E}_{\mathbb{D}}[\text{Regret}(\hat{\pi}, \lambda(\cdot))] &\lesssim \min \left(V_{max}, V_{max} \sqrt{\frac{(1-\gamma)|\mathcal{S}| \max_{s,a} \frac{d^{\pi^*}(s,a;d_0)}{\mu(s,a)}}{N(1-\gamma(1-\lambda))^4}} \right) \\ &\quad + \frac{\gamma\lambda}{1-\gamma} \min \left(V_{max}, V_{max} \sqrt{\frac{(1-\gamma)|\mathcal{S}| \frac{1}{\min_{(s,a) \in \Omega} \mu(s,a)}}{N(1-\gamma(1-\lambda))^4}} \right). \end{aligned}$$

□

B.2 Proof of Theorem 2

The proof follows by combining Lemma 7 and 9.

C VI-LCB with HUBL

We use the offline value iteration with lower confidence bound (VI-LCB) [Rashidinejad et al., 2021] as the base algorithm to analyze concretely the effects of HUBL with finite samples for the tabular case.

Algorithm 4 HUBL with VI-LCB

- 1: **Input:** Batch dataset \mathbb{D} and discount factor γ .
- 2: Set $T := \frac{\log N}{1-\gamma}$.
- 3: Randomly split \mathbb{D} into $T + 1$ sets $\mathbb{D}_t = \{(s_i, a_i, r_i, s'_i)\}$ for $t \in \{0, 1, \dots, T\}$, where D_0 consists of $\frac{N}{2}$ observations and other datasets have $\frac{N}{2T}$ observations.
- 4: Set $m_0(s, a) := \sum_{i=1}^m \mathbb{1}\{(s_i, a_i) = (s, a)\}$ based on dataset \mathbb{D}_0 .
- 5: For all $a \in \mathcal{A}$ and $s \in \mathcal{S}$, initialize $Q_0(s, a) = 0$, $V_0(s) = 0$ and set $\pi_0(s) = \arg \max_a m_0(s, a)$.
- 6: **for** $t = 1, \dots, T$ **do**
- 7: Initialize $r_t(s, a) = 0$ and set $P_{s,a}^t$ to be a random probability vector.
- 8: Set $m_t(s, a) := \sum_{i=1}^m \mathbb{1}\{(s_i, a_i) = (s, a)\}$ based on dataset \mathbb{D}_t .
- 9: Compute penalty $b_t(s, a)$ for $L = 2000 \log(2(T+1)|\mathcal{S}||\mathcal{A}|N)$

$$b_t(s, a) := V_{\max} \sqrt{\frac{L}{m_t(s, a) \vee 1}}.$$

- 10: **for** $(s, a) \in (\mathcal{S}, \mathcal{A})$ **do**
 - 11: **if** $m_t(s, a) \geq 1$ **then**
 - 12: Set $P_{s,a}^t$ to be empirical transitions and $r_t(s, a)$ be empirical average of rewards.
 - 13: **end if**
 - 14: Set $Q_t(s, a) \leftarrow r_t(s, a) - b_t(s, a) + \gamma P_{s,a}^t \odot (I - \Lambda_{s,:}) \cdot V_{t-1} + \gamma P_{s,a}^t \odot \Lambda_{s,:} \cdot h$.
 - 15: **end for**
 - 16: Compute $V_t^{mid}(s) \leftarrow \max_a Q_t(s, a)$ and $\pi_t^{mid}(s) \in \arg \max_a Q_t(s, a)$.
 - 17: **for** $s \in \mathcal{S}$ **do**
 - 18: **if** $V_t^{mid}(s) \leq V_{t-1}(s)$ **then**
 - 19: $V_t(s) \leftarrow V_{t-1}(s)$ and $\pi_t(s) \leftarrow \pi_{t-1}(s)$.
 - 20: **else**
 - 21: $V_t(s) \leftarrow V_t^{mid}(s)$ and $\pi_t(s) \leftarrow \pi_t^{mid}(s)$.
 - 22: **end if**
 - 23: **end for**
 - 24: **end for**
 - 25: **Return** $\hat{\pi} := \pi_T$.
-

C.1 Algorithm

We detail the procedure of HUBL when implemented with VI-LCB for the tabular setting. To start with, we introduce several definitions which will be used in the following algorithm and theoretical analysis. Without loss of generality, we assume that the states take values in $\{1, 2, \dots, |\mathcal{S}|\}$ and that the actions take values in $\{1, 2, \dots, |\mathcal{A}|\}$. Then, let h be a $|\mathcal{S}| \times 1$ vector which denotes the heuristic function. We assume each component satisfies $h_s = V^\mu(s)$ for $s \in \Omega$. Let Λ be a $|\mathcal{S}| \times |\mathcal{S}|$ matrix with $\Lambda_{s,s'} = \lambda$ if $s, s' \in \Omega$ and $\Lambda_{s,s'} = 0$ if s or $s' \notin \Omega$. We use \odot to denote the component-wise multiplication, and $\Lambda_{s,:}$ to denote a row of Λ as a $|\mathcal{S}| \times 1$ vector. With slight abuse of notation, we use t to denote the index of iteration in this section, with T as the total number of iterations.

To conduct VI-LCB with HUBL, we follow Algorithm 3 in Rashidinejad et al. [2021] but with a modified updating rule. The procedure is summarized Algorithm 4. Compared with the original VI-LCB, we highlight the key modification in Line 14 with blue color. Specifically, at the t^{th} iteration, based on (2), we modify updating rule of Algorithm 3 in Rashidinejad et al. [2021] into

$$Q_t(s, a) \leftarrow r_t(s, a) - b_t(s, a) + \gamma P_{s,a}^t \odot (I - \Lambda_{s,:}) \cdot V_{t-1} + \gamma P_{s,a}^t \odot \Lambda_{s,:} \cdot h.$$

Note that we introduce heuristics by $\gamma P_{s,a}^t \odot \Lambda_{s,:} \cdot h$, while reducing the bootstrapping by $\gamma P_{s,a}^t \odot (I - \Lambda_{s,:}) \cdot V_{t-1}$.

C.2 Regret Analysis

In this section, we study the regret under the reshaped MDP constructed by HUBL. Specifically, we bound the regret of Algorithm 4 in Lemma 10.

Lemma 10 (Regret of VI-LCB with HUBL). *Let the assumptions in Section C.3 be satisfied. Then, for any initial distribution d_{init} in Ω , the regret of Algorithm 4 is bounded by*

$$\mathbb{E}_{\mathbb{D}}[\tilde{V}^{\pi^*}(d_{init}) - \tilde{V}^{\hat{\pi}}(d_{init})] \lesssim \min \left(V_{max}, V_{max} \sqrt{\frac{(1-\gamma)|\mathcal{S}| \max_{s,a} \frac{d^{\pi^*}(s,a;d_{init})}{\mu(s,a)}}{N(1-\gamma(1-\lambda))^4}} \right).$$

C.3 Notations

We first provide some matrix notations for MDPs. We use $P^\pi \in \mathbb{R}^{|\mathcal{S}||\mathcal{A}| \times |\mathcal{S}||\mathcal{A}|}$ to denote the transition matrix induced by policy π whose $(s, a) \times (s', a')$ element is equal to $P(s'|s, a)\pi(a'|s')$, and $d^\pi \in \mathbb{R}^{|\mathcal{S}||\mathcal{A}|}$ to denote a state-action distribution induced by policy π whose (s, a) element is equal to $d(s)\pi(a|s)$. Similarly, we use $\Lambda_Q \in \mathbb{R}^{|\mathcal{S}||\mathcal{A}| \times |\mathcal{S}||\mathcal{A}|}$ to denote an extended matrix version of Λ .

Further, we focus on the policies which stay in the data distribution support Ω . Such policies are formally defined as $\{\pi | d^\pi(s, a; s_0) = 0 \text{ for any } (s, a) \notin \Omega \text{ and } s_0 \in \Omega\}$. We also define a clean event:

$$\mathcal{E}_{MDP} := \left\{ \forall s, a, t, |r(s, a) - r_t(s, a) + \gamma(P_{s,a} - P_{s,a}^t) \odot (I - \Lambda) \cdot V_{t-1}| \leq b_t(s, a) \right\}.$$

C.4 Technical Lemmas

With the aforementioned definitions and assumptions, we provide the following lemmas.

Lemma 11. *Let π be a policy learned by Algorithm 4. Under the event $\mathcal{E}_{cover} := \{\Omega \subseteq \mathbb{D}_0\}$ π stays in Ω for any initial state in Ω . The probability of \mathcal{E}_{cover} is greater than*

$$1 - |\mathcal{S}|(1 - \min_{s \in \Omega} \mu(s))^{\frac{N}{2}}.$$

Proof. Under the event \mathcal{E}_{cover} , we first fix $s \in \Omega$ and show that given s , the learned policy π does not take any action $a' \notin \Omega$. By Algorithm 4, for any $(s, a') \notin \Omega$ and $t = 1, 2, \dots, T$, we can derive

$$Q_t(s, a') \leq -V_{max} \sqrt{2000 \log(2T+1)} |\mathcal{S}| |\mathcal{A}| N + \gamma V_{max}.$$

Since N and T are larger than 1, we can conclude that

$$Q_t(s, a') \leq 0 \text{ for any } a' \text{ such that } (s, a') \notin \Omega.$$

Next we consider two cases:

Case I: If there exists a such that $(s, a) \in \Omega$ and that there exists $t = 1, 2, \dots, T$ such that

$$Q_t(s, a) > 0,$$

we can conclude that $Q_T(s, a) \geq Q_t(s, a) > Q(s, a')$, which suggests that the learned policy π never conducts action $a' \notin \Omega$ given state s .

Case II: If for any a such that $(s, a) \in \Omega$ and any $t = 1, 2, \dots, T$, we have

$$Q_t(s, a) = 0,$$

according to Algorithm 4, $\pi(s) = \arg \max_a m_0(s, a)$. By the definition of \mathcal{E}_{cover} , the policy π stays in Ω .

Next, we consider the probability of \mathcal{E}_{cover} . Given a state $s \in \Omega$, we define the event $\mathcal{E}_s := \{m_0(s, a) = 0 \text{ for all } a \text{ such that } (s, a) \in \Omega\}$. The probability of \mathcal{E}_s can be derived as

$$\mathbb{P}(\mathcal{E}_s) \leq (1 - \mu(s))^{\frac{N}{2}}.$$

By union bound, we can derive that

$$\mathbb{P}(\neg \mathcal{E}_{cover}) \leq |\mathcal{S}|(1 - \min_{s \in \Omega} \mu(s))^{\frac{N}{2}}.$$

As a result, π stays in Ω with the probability greater than

$$1 - |\mathcal{S}|(1 - \min_{s \in \Omega} \mu(s))^{\frac{N}{2}}.$$

□

Lemma 12. Let π be a policy that stays in Ω . Then, with d_{init} as any initial distribution in Ω , we can derive

$$\frac{d_{init}(s)}{\mu(s, \pi(s))} \leq \frac{\tilde{d}^\pi(s, \pi(s); d_{init})}{1 - \gamma(1 - \lambda)}.$$

Proof. By definition, we have

$$\tilde{d}^\pi(s, \pi(s); d_{init}(s)) := \frac{1}{1 - \gamma(1 - \lambda)} \sum_{t=0}^{\infty} \gamma^t (1 - \lambda)^t \mathbf{P}_t(S_t = s, \pi; d_{init})$$

Therefore, $d_{init}(s) \leq \frac{1}{1 - \gamma(1 - \lambda)} \tilde{d}^\pi(s, \pi(s); d_{init})$, which finishes the proof. \square

Lemma 13. Let $v_k^\pi = d_{init}^\pi(\gamma P^\pi \odot (I - \Lambda_Q))^k$. For a policy π that stays in Ω , the following equality holds: $v_k^\pi = d_{init}^\pi(\gamma(1 - \lambda)P^\pi)^k$.

Proof. Since π stays in Ω , P^π only accesses the entries in $I - \Lambda_Q$ whose values equal to $(1 - \lambda)$. This observation finishes the proof. \square

Lemma 14. Let π be a policy that stays in Ω . Under the event \mathcal{E}_{MDP} , for all $t = 1, 2, \dots, T$,

$$\tilde{V}(\pi) - \tilde{V}(\pi_t) \leq V_{max} \gamma^t (1 - \lambda)^t + 2 \sum_{i=1}^t \mathbb{E}_{v_{t-i}^\pi} [b_i(s, a)].$$

Proof. The proof follows the Lemma 2 of Rashidinejad et al. [2021] combined with Lemma 13. \square

Lemma 15. For any policy π that stays in Ω , the following inequality is true:

$$\tilde{d}^\pi(s, a; d_{init}) \leq \frac{1 - \gamma}{1 - \gamma(1 - \lambda)} d^\pi(s, a; d_{init}),$$

for any $(s, a) \in \Omega$.

Proof. By definition, we have

$$\begin{aligned} \tilde{d}^\pi(s, a; d_{init}) &:= \frac{1}{1 - \gamma(1 - \lambda)} \sum_{t=0}^{\infty} \gamma^t (1 - \lambda)^t \mathbf{P}_t(S_t = s, A_t = a; \pi, d_{init}) \\ d^\pi(s, a; d_{init}) &:= \frac{1}{1 - \gamma} \sum_{t=0}^{\infty} \gamma^t \mathbf{P}_t(S_t = s, A_t = a; \pi, d_{init}). \end{aligned}$$

Therefore,

$$\tilde{d}^\pi(s, a; d_{init}) \leq \frac{1}{1 - \gamma(1 - \lambda)} \sum_{t=0}^{\infty} \gamma^t \mathbf{P}_t(S_t = s, A_t = a; \pi, d_{init}) = \frac{1 - \gamma}{1 - \gamma(1 - \lambda)} d^\pi(s, a; d_{init})$$

\square

C.5 Proof of Lemma 10

By the event \mathcal{E}_{cover} , we can decompose the regret into

$$\begin{aligned} &\mathbb{E}_{\mathbb{D}}[\tilde{V}^{\pi^*}(d_{init}) - \tilde{V}^{\hat{\pi}}(d_{init})] \\ &\leq \mathbb{E}_{\mathbb{D}}[\tilde{V}^{\pi^*}(d_{init}) - \tilde{V}^{\hat{\pi}}(d_{init}) \mathbb{1}\{\mathcal{E}_{cover}\}] + \mathbb{E}_{\mathbb{D}}[\tilde{V}^{\pi^*}(d_{init}) - \tilde{V}^{\hat{\pi}}(d_{init}) \mathbb{1}\{\mathcal{E}_{cover}^c\}] \\ &\leq \mathbb{E}_{\mathbb{D}}[\tilde{V}^{\pi^*}(d_{init}) - \tilde{V}^{\hat{\pi}}(d_{init}) \mathbb{1}\{\mathcal{E}_{cover}\}] + V_{max} |\mathcal{S}| \left(\frac{|\mathcal{S}| - 1}{|\mathcal{S}|} \right)^{\frac{N}{2}}, \end{aligned} \quad (10)$$

where the second inequality is by Lemma 11. Next, we focus on $\mathbb{E}_{\mathbb{D}}[\tilde{V}^{\pi^*}(d_{init}) - \tilde{V}^{\hat{\pi}}(d_{init}) \mathbb{1}\{\mathcal{E}_{cover}\}]$. Following the analysis in C.5 of Rashidinejad et al. [2021], we can derive

$$\begin{aligned}
& \mathbb{E}_{\mathbb{D}}[(\tilde{V}^{\pi^*}(d_{init}) - \tilde{V}^{\hat{\pi}}(d_{init})) \mathbb{1}\{\mathcal{E}_{cover}\}] \\
& \leq \mathbb{E}_{\mathbb{D}}[(\tilde{V}^{\pi^*}(d_{init}) - \tilde{V}^{\hat{\pi}}(d_0)) \mathbb{1}\{\mathcal{E}_{cover}\}] \\
& \leq \mathbb{E}_{\mathbb{D}}[\mathbb{E}_{s \sim d_{init}}[(\tilde{V}^{\pi^*}(d_{init}) - \tilde{V}^{\hat{\pi}}(d_{init})) \mathbb{1}\{\exists t \leq T, m_t(s, \pi^*(s)) = 0\} \mathbb{1}\{\mathcal{E}_{cover}\}]] := T_1 \\
& \quad + \mathbb{E}_{\mathbb{D}}[\mathbb{E}_{s \sim d_{init}}[(\tilde{V}^{\pi^*}(d_{init}) - \tilde{V}^{\hat{\pi}}(d_{init})) \\
& \quad \mathbb{1}\{\forall t \leq T, m_t(s, \pi^*(s)) \geq 1\} \mathbb{1}\{\mathcal{E}_{MDP}\} \mathbb{1}\{\mathcal{E}_{cover}\}]] := T_2 \\
& \quad + \mathbb{E}_{\mathbb{D}}[\mathbb{E}_{s \sim d_{init}}[(\tilde{V}^{\pi^*}(d_{init}) - \tilde{V}^{\hat{\pi}}(d_{init})) \\
& \quad \mathbb{1}\{\forall t \leq T, m_t(s, \pi^*(s)) \geq 1\} \mathbb{1}\{\mathcal{E}_{MDP}^c\} \mathbb{1}\{\mathcal{E}_{cover}\}]] := T_3.
\end{aligned}$$

By Lemma 11, under the event \mathcal{E}_{cover} , $\hat{\pi}$ stays in Ω . In other words, Lemma 12, 13 and 14 are all applicable to $\hat{\pi}$.

Next, for the following analysis, we consider the case that π^* stays in Ω . We will discuss the case that Ω does not cover π^* at the end of the proof.

By Lemma 12 and C.5.1 of Rashidinejad et al. [2021],

$$T_1 \leq \frac{8V_{max}|\mathcal{S}|T^2 \max_{s,a} \frac{\tilde{d}^{\pi^*}(s,a;d_{init})}{\mu(s,a)}}{9(1 - (1 - \lambda)\gamma)N}.$$

By Lemma 14 and C.5.2 of Rashidinejad et al. [2021],

$$T_2 \leq V_{max}\gamma^T(1 - \lambda)^T + 32\frac{V_{max}}{1 - \gamma(1 - \lambda)}\sqrt{\frac{2L|\mathcal{S}|T \max_{s,a} \frac{\tilde{d}^{\pi^*}(s,a;d_{init})}{\mu(s,a)}}{N}}.$$

By C.5.2 of Rashidinejad et al. [2021],

$$T_3 \leq \frac{V_{max}}{N}.$$

Combining T_1, T_2, T_3 , and (10), with $T = \log N / (1 - \gamma(1 - \lambda))$,

$$\mathbb{E}_{\mathbb{D}}[\tilde{V}^{\pi^*}(d_{init}) - \tilde{V}^{\hat{\pi}}(d_{init})] \lesssim \min\left(V_{max}, V_{max}\sqrt{\frac{|\mathcal{S}| \max_{s,a} \frac{\tilde{d}^{\pi^*}(s,a;d_{init})}{\mu(s,a)}}{N(1 - \gamma(1 - \lambda))^3}}\right).$$

Finally, by Lemma 15, we finish the proof:

$$\mathbb{E}_{\mathbb{D}}[\tilde{V}^{\pi^*}(d_{init}) - \tilde{V}^{\hat{\pi}}(d_{init})] \lesssim \min\left(V_{max}, V_{max}\sqrt{\frac{(1 - \gamma)|\mathcal{S}| \max_{s,a} \frac{\tilde{d}^{\pi^*}(s,a;d_{init})}{\mu(s,a)}}{N(1 - \gamma(1 - \lambda))^4}}\right). \quad (11)$$

Note that (11) is derived under the assumption that π^* stays in Ω . However, it also holds when π^* is not covered by Ω . In that case, $\max_{s,a} \frac{\tilde{d}^{\pi^*}(s,a;d_{init})}{\mu(s,a)} = \infty$ and $\mathbb{E}_{\mathbb{D}}[\tilde{V}^{\pi^*}(d_{init}) - \tilde{V}^{\hat{\pi}}(d_{init})] \leq V_{max}$.

D Extended Results for Experiments

We conduct HUBL with four offline RL base methods on 27 datasets in D4RL and Meta-World. By blending heuristics with bootstrapping, HUBL reduces the complexity of decision-making and provides smaller regret while generating limited bias. We demonstrate that HUBL is able to improve the performance of offline RL methods.

D.1 Implementation Details

We implement base offline RL methods with code sources provided in Table 3.

Table 3: Code source for base methods.

Base Methods	Code Source
ATAC	https://github.com/chinganc/lightATAC
CQL	https://github.com/young-geng/CQL/tree/master/SimpleSAC
IQL	https://github.com/gwthomas/IQL-PyTorch/blob/main/README.md
TD3+BC	https://github.com/sfujim/TD3_BC

Experiments with ATAC, IQL, and TD3+BC are ran on Standard_F4S_V2 nodes of Azure, and experiments with CQL are ran on NC6S_V2 nodes of Azure. As suggested by the original implementation of the considered base offline RL methods, we use 3-layer fully connected neural networks for policy critics and value networks, where each hidden layer has 256 neurons and ReLU activation and the output layer is linear. The first-order optimization is implemented by ADAM [Kingma and Ba, 2014] with a minibatch size as 256. The learning rates are selected following the original implementation and are reported in Table 4.

Table 4: Learning rates

Base Methods	Policy Network	Q Network
ATAC	5×10^{-7}	5×10^{-4}
CQL	3×10^{-4}	3×10^{-4}
IQL	3×10^{-4}	3×10^{-4}
TD3_BC	3×10^{-4}	3×10^{-4}

For each dataset, the hyperparameters of base methods are tuned from six different configurations suggested by the original papers. Such configurations are summarized in Table 5.

Table 5: Learning rates

Base Methods	Hyperparameter	Values
ATAC	degree of pessimism β	{1.0, 4.0, 16.0, 0.25, 0.625, 10}
CQL	min Q weight	{5, 20, 80, 1.25, 0.3125, 10.0}
IQL	inverse temperature β	{6.5, 3.0, 10.0}
	expectile parameter τ	{0.7, 0.9}
TD3+BC	strength of the regularizer λ	{2.5, 0.625, 10.0, 40.0, 0.15625, 1}

Meanwhile, HUBL has one extra hyperparameter, α , which is *fixed* for all the datasets but different for each base method. Specifically, α is selected from {0.001, 0.01, 0.1} according to the relative improvement averaged over all the datasets in one task. Later in the robustness analysis, we show that the performance of HUBL is insensitive to the selection of α . For each configuration and each base method, we repeat experiments three times with seeds in {0, 1, 10}.

D.2 Base Performance and Standard Deviations for D4RL Datasets

We provide the performance of base offline RL methods and standard deviations in Table 6.

Table 6: Relative normalized score improvement for HUBL and normalized scores of base methods on D4RL datasets.

	Sigmoid	Rank	Constant	ATAC
halfcheetah-medium-expert-v2	0.02 ± 0.0	0.02 ± 0.01	0.02 ± 0.0	92.5 ± 0.73
halfcheetah-medium-replay-v2	0.01 ± 0.01	0.02 ± 0.01	0.02 ± 0.02	46.89 ± 0.25
halfcheetah-medium-v2	-0.0 ± 0.01	0.0 ± 0.0	0.02 ± 0.01	52.54 ± 0.63
hopper-medium-expert-v2	0.0 ± 0.0	0.0 ± 0.0	0.0 ± 0.0	111.04 ± 0.13
hopper-medium-replay-v2	0.0 ± 0.0	0.0 ± 0.01	0.0 ± 0.0	101.23 ± 0.59
hopper-medium-v2	0.01 ± 0.04	0.02 ± 0.07	-0.03 ± 0.15	85.59 ± 4.76
walker2d-medium-expert-v2	0.0 ± 0.0	0.02 ± 0.0	0.0 ± 0.01	111.99 ± 0.8
walker2d-medium-replay-v2	0.03 ± 0.03	0.08 ± 0.0	0.05 ± 0.08	84.22 ± 2.7
walker2d-medium-v2	0.01 ± 0.01	-0.02 ± 0.05	0.02 ± 0.0	87.2 ± 0.67
Average Relative Improvement	0.01	0.02	0.01	-
	Sigmoid	Rank	Constant	CQL
halfcheetah-medium-expert-v2	0.02 ± 0.02	0.03 ± 0.06	-0.02 ± 0.17	81.96 ± 9.93
halfcheetah-medium-replay-v2	0.1 ± 0.01	0.18 ± 0.02	0.13 ± 0.01	40.98 ± 0.81
halfcheetah-medium-v2	-0.1 ± 0.01	-0.02 ± 0.01	-0.03 ± 0.01	51.05 ± 0.83
hopper-medium-expert-v2	0.42 ± 0.01	0.39 ± 0.07	0.38 ± 0.05	78.39 ± 14.51
hopper-medium-replay-v2	0.03 ± 0.01	0.01 ± 0.01	0.02 ± 0.01	97.21 ± 3.15
hopper-medium-v2	0.18 ± 0.14	0.15 ± 0.17	0.17 ± 0.06	70.27 ± 8.77
walker2d-medium-expert-v2	0.21 ± 0.0	0.22 ± 0.01	0.22 ± 0.0	89.38 ± 17.54
walker2d-medium-replay-v2	0.08 ± 0.27	0.38 ± 0.06	0.37 ± 0.04	63.35 ± 6.22
walker2d-medium-v2	0.05 ± 0.05	0.05 ± 0.03	-0.03 ± 0.15	79.41 ± 1.82
Average Relative Improvement	0.11	0.16	0.13	-
	Sigmoid	Rank	Constant	IQL
halfcheetah-medium-expert-v2	0.0 ± 0.01	0.0 ± 0.0	-0.05 ± 0.03	92.92 ± 0.5
halfcheetah-medium-replay-v2	-0.03 ± 0.02	0.0 ± 0.02	-0.04 ± 0.03	44.35 ± 0.21
halfcheetah-medium-v2	-0.01 ± 0.0	0.0 ± 0.0	-0.01 ± 0.01	49.61 ± 0.16
hopper-medium-expert-v2	-0.04 ± 0.03	-0.03 ± 0.02	-0.09 ± 0.12	108.13 ± 2.69
hopper-medium-replay-v2	0.72 ± 0.09	0.58 ± 0.25	0.62 ± 0.27	53.98 ± 4.18
hopper-medium-v2	0.03 ± 0.03	0.02 ± 0.03	-0.01 ± 0.15	61.03 ± 3.27
walker2d-medium-expert-v2	0.01 ± 0.0	0.01 ± 0.01	0.01 ± 0.0	109.59 ± 0.2
walker2d-medium-replay-v2	0.15 ± 0.12	0.21 ± 0.02	0.13 ± 0.04	73.57 ± 2.64
walker2d-medium-v2	0.03 ± 0.02	0.03 ± 0.01	0.04 ± 0.01	81.68 ± 2.48
Average Relative Improvement	0.09	0.09	0.06	-
	Sigmoid	Rank	Constant	TD3+BC
halfcheetah-medium-expert-v2	-0.02 ± 0.03	-0.02 ± 0.03	-0.02 ± 0.02	94.82 ± 0.33
halfcheetah-medium-replay-v2	-0.1 ± 0.03	-0.08 ± 0.16	-0.0 ± 0.02	54.38 ± 1.24
halfcheetah-medium-v2	-0.07 ± 0.02	-0.04 ± 0.01	-0.01 ± 0.01	64.63 ± 2.15
hopper-medium-expert-v2	-0.06 ± 0.13	-0.16 ± 0.2	0.03 ± 0.05	98.79 ± 12.57
hopper-medium-replay-v2	0.16 ± 0.08	0.21 ± 0.03	0.24 ± 0.03	81.43 ± 27.77
hopper-medium-v2	0.51 ± 0.17	0.7 ± 0.02	0.6 ± 0.19	59.12 ± 3.39
walker2d-medium-expert-v2	0.0 ± 0.01	0.01 ± 0.01	0.0 ± 0.0	111.87 ± 0.17
walker2d-medium-replay-v2	0.12 ± 0.04	0.09 ± 0.07	0.05 ± 0.02	84.95 ± 1.85
walker2d-medium-v2	-0.01 ± 0.03	0.08 ± 0.01	0.0 ± 0.07	84.09 ± 1.94
Average Relative Improvement	0.06	0.09	0.1	-

D.3 Robustness of HUBL to α

In this section, we demonstrate the robustness of HUBL to α . Specifically, we provide the average relative improvements of HUBL on D4RL datasets in Table 7. Notice that most average relative improvements are positive, which shows that HUBL can improve the performance with different values.

Table 7: Average relative improvements of HUBL under different α 's

	Sigmoid	Rank	Constant
$\alpha = 0.001$	0.01	0.01	0
$\alpha = 0.01$	0.01	0.01	0.01
$\alpha = 0.1$	0	0.02	0.01

(a) ATAC

	Sigmoid	Rank	Constant
$\alpha = 0.001$	0.05	0.05	0.03
$\alpha = 0.01$	0.08	0.05	0.10
$\alpha = 0.1$	0.11	0.16	0.13

(b) CQL

	Sigmoid	Rank	Constant
$\alpha = 0.001$	0.02	0	-0.04
$\alpha = 0.01$	0	-0.01	-0.02
$\alpha = 0.1$	0.09	0.09	0.06

(c) IQL

	Sigmoid	Rank	Constant
$\alpha = 0.001$	0.01	0.01	0
$\alpha = 0.01$	0.01	0.01	0.01
$\alpha = 0.1$	0.06	0.09	0.06

(d) TD3_BC

The selected α 's are reported in Table 8:

Table 8: Selected α 's

	Sigmoid	Rank	Constant
ATAC	0.01	0.01	0.1
CQL	0.1	0.1	0.1
IQL	0.1	0.1	0.1
TD3_BC	0.01	0.1	0.1

D.4 Data Collection for Meta-World

We collect data for Meta-World tasks using normalized rewards with goal-oriented stopping. Specifically, given that the original rewards of Meta-World are in $[0, 10]$, we shift them by -10 and divide by 10, so that the normalized rewards take values in $[-1, 0]$. Then, we use the hand scripted policy given in Meta-World with different Gaussian noise levels in $\{0.1, 0.5, 1\}$ to collect 100 trajectory for each task. In this process, a trajectory ends if (i) it reaches the max length of a trajectory (150); (ii) it finishes the goal. Note that we follow the same rule when testing the performance of a learned policy.

D.5 Base Performance and Standard Deviations for Meta-World Datasets

We provide the performance of base offline RL methods and standard deviations in Table 9 and 10. We also consider behavior cloning (BC) as a baseline, and also a representative for imitation learning and inverse reinforcement learning methods [Fu et al., 2017, Geng et al., 2020, 2023]. Since the behavior policy is the scripted policy with Gaussian noise, BC can effectively recover the scripted policy and thus is especially competitive.

Table 9: Relative normalized score improvement for HUBL and normalized scores of base methods on MW datasets (part I)

	Sigmoid	Rank	Constant	ATAC	BC
button-press-v2-noise0.1	-0.0 ± 0.03	0.01 ± 0.01	0.01 ± 0.01	-58.12 ± 0.45	-58.79
button-press-v2-noise0.5	-0.0 ± 0.03	-0.03 ± 0.05	0.01 ± 0.04	-64.16 ± 0.93	-59.58
button-press-v2-noise1	-0.05 ± 0.07	-0.0 ± 0.04	-0.01 ± 0.04	-62.72 ± 3.84	-61.24
push-back-v2-noise0.1	0.1 ± 0.03	0.04 ± 0.07	0.15 ± 0.06	-87.12 ± 13.89	-104.85
push-back-v2-noise0.5	0.11 ± 0.07	0.19 ± 0.05	0.17 ± 0.02	-133.28 ± 14.24	-134.63
push-back-v2-noise1	0.04 ± 0.05	0.02 ± 0.09	0.06 ± 0.07	-141.29 ± 13.87	-143.63
reach-v2-noise0.1	-0.0 ± 0.06	-0.0 ± 0.05	0.0 ± 0.07	-17.19 ± 0.76	-18.31
reach-v2-noise0.5	0.37 ± 0.07	0.46 ± 0.06	0.43 ± 0.08	-33.91 ± 5.62	-24.57
reach-v2-noise1	0.39 ± 0.05	0.35 ± 0.24	0.5 ± 0.05	-46.58 ± 3.98	-43.79
Average Relative Improvement	0.11	0.11	0.14	-	-
	Sigmoid	Rank	Constant	CQL	BC
button-press-v2-noise0.1	0.0 ± 0.03	0.02 ± 0.05	0.03 ± 0.03	-59.67 ± 1.69	-58.79
button-press-v2-noise0.5	-0.04 ± 0.05	-0.02 ± 0.01	-0.02 ± 0.0	-58.48 ± 0.85	-59.58
button-press-v2-noise1	-0.08 ± 0.12	0.08 ± 0.02	0.04 ± 0.11	-67.18 ± 14.25	-61.24
push-back-v2-noise0.1	-0.07 ± 0.07	0.02 ± 0.05	0.02 ± 0.02	-81.78 ± 2.88	-104.85
push-back-v2-noise0.5	0.25 ± 0.12	0.22 ± 0.1	0.19 ± 0.12	-124.64 ± 2.45	-134.63
push-back-v2-noise1	0.06 ± 0.13	0.11 ± 0.14	0.1 ± 0.05	-133.66 ± 8.17	-143.63
reach-v2-noise0.1	-0.04 ± 0.17	-0.01 ± 0.05	-0.04 ± 0.02	-18.5 ± 2.52	-18.31
reach-v2-noise0.5	0.51 ± 0.05	0.18 ± 0.53	0.4 ± 0.27	-41.02 ± 18.79	-24.57
reach-v2-noise1	0.8 ± 0.02	0.35 ± 0.15	0.81 ± 0.03	-107.14 ± 32.75	-43.79
Average Relative Improvement	0.16	0.1	0.17	-	-
	Sigmoid	Rank	Constant	IQL	BC
button-press-v2-noise0.1	0.02 ± 0.02	0.03 ± 0.01	0.03 ± 0.01	-59.87 ± 1.32	-58.79
button-press-v2-noise0.5	-0.01 ± 0.05	-0.01 ± 0.02	-0.14 ± 0.13	-60.68 ± 0.29	-59.58
button-press-v2-noise1	-0.09 ± 0.15	0.07 ± 0.01	0.04 ± 0.03	-73.96 ± 5.09	-61.24
push-back-v2-noise0.1	0.01 ± 0.04	0.04 ± 0.02	0.03 ± 0.01	-83.79 ± 5.45	-104.85
push-back-v2-noise0.5	0.02 ± 0.06	0.04 ± 0.05	-0.03 ± 0.05	-124.86 ± 7.45	-134.63
push-back-v2-noise1	0.0 ± 0.01	0.03 ± 0.04	-0.0 ± 0.02	-143.26 ± 6.31	-143.63
reach-v2-noise0.1	-0.03 ± 0.03	-0.06 ± 0.03	-0.04 ± 0.07	-17.37 ± 0.87	-18.31
reach-v2-noise0.5	0.05 ± 0.13	-0.02 ± 0.03	-0.02 ± 0.24	-31.51 ± 9.39	-24.57
reach-v2-noise1	-0.12 ± 0.42	0.05 ± 0.09	0.01 ± 0.37	-42.23 ± 7.4	-43.79
Average Relative Improvement	-0.02	0.02	-0.01	-	-
	Sigmoid	Rank	Constant	TD3+BC	BC
button-press-v2-noise0.1	0.25 ± 0.0	0.23 ± 0.0	0.23 ± 0.02	-77.68 ± 22.14	-58.79
button-press-v2-noise0.5	-0.04 ± 0.05	-0.04 ± 0.06	-0.09 ± 0.07	-59.54 ± 1.68	-59.58
button-press-v2-noise1	0.02 ± 0.07	0.12 ± 0.23	0.1 ± 0.12	-81.03 ± 5.79	-61.24
push-back-v2-noise0.1	0.08 ± 0.01	-0.01 ± 0.02	0.05 ± 0.04	-85.44 ± 5.05	-104.85
push-back-v2-noise0.5	0.07 ± 0.07	0.05 ± 0.14	0.05 ± 0.1	-127.95 ± 9.82	-134.63
push-back-v2-noise1	0.01 ± 0.04	0.01 ± 0.06	-0.04 ± 0.02	-139.72 ± 15.6	-143.63
reach-v2-noise0.1	-0.06 ± 0.04	-0.02 ± 0.02	-0.0 ± 0.02	-17.11 ± 1.28	-18.31
reach-v2-noise0.5	0.12 ± 0.19	0.25 ± 0.14	0.15 ± 0.18	-40.69 ± 9.66	-24.57
reach-v2-noise1	0.13 ± 0.18	0.04 ± 0.12	0.1 ± 0.11	-65.48 ± 2.85	-43.79
Average Relative Improvement	0.07	0.07	0.06	-	-

Table 10: Relative normalized score improvement for HUBL and normalized scores of base methods on MW datasets (part II)

	Sigmoid	Rank	Constant	ATAC	BC
assembly-v2-noise0.1	-0.01 ± 0.03	0.01 ± 0.04	-0.0 ± 0.08	-70.22 ± 4.61	-71.76
assembly-v2-noise0.5	0.01 ± 0.02	0.03 ± 0.02	0.08 ± 0.05	-135.77 ± 1.58	-129.53
assembly-v2-noise1	-0.01 ± 0.01	0.02 ± 0.01	0.04 ± 0.01	-140.12 ± 2.45	-138.63
handle-press-side-v2-noise0.1	-0.03 ± 0.01	-0.02 ± 0.02	-0.03 ± 0.03	-32.38 ± 0.64	-36.28
handle-press-side-v2-noise0.5	0.0 ± 0.03	0.02 ± 0.03	-0.01 ± 0.03	-33.04 ± 0.96	-34.3
handle-press-side-v2-noise1	0.04 ± 0.12	-0.02 ± 0.1	-0.09 ± 0.06	-35.33 ± 3.7	-35.72
plate-slide-back-side-v2-noise0.1	-0.0 ± 0.04	-0.03 ± 0.02	0.02 ± 0.05	-37.07 ± 0.87	-37.75
plate-slide-back-side-v2-noise0.5	0.07 ± 0.41	0.17 ± 0.29	0.15 ± 0.02	-68.9 ± 10.92	-65.47
plate-slide-back-side-v2-noise1	0.17 ± 0.3	0.43 ± 0.02	0.44 ± 0.11	-97.9 ± 25.46	-128.28
Average Relative Improvement	0.03	0.07	0.07	-	-
	Sigmoid	Rank	Constant	CQL	BC
assembly-v2-noise0.1	0.03 ± 0.06	0.06 ± 0.17	0.06 ± 0.07	-76.29 ± 9.41	-71.76
assembly-v2-noise0.5	-0.0 ± 0.02	0.01 ± 0.04	-0.01 ± 0.02	-131.35 ± 2.62	-129.53
assembly-v2-noise1	-0.0 ± 0.03	-0.0 ± 0.01	0.0 ± 0.02	-138.94 ± 0.97	-138.63
handle-press-side-v2-noise0.1	0.11 ± 0.07	-0.02 ± 0.07	0.02 ± 0.19	-34.47 ± 4.54	-36.28
handle-press-side-v2-noise0.5	0.32 ± 0.11	0.38 ± 0.11	0.46 ± 0.01	-70.96 ± 29.39	-34.3
handle-press-side-v2-noise1	0.15 ± 0.12	0.13 ± 0.2	0.4 ± 0.05	-55.3 ± 33.42	-35.72
plate-slide-back-side-v2-noise0.1	0.05 ± 0.03	-0.0 ± 0.11	0.03 ± 0.11	-36.31 ± 2.33	-37.75
plate-slide-back-side-v2-noise0.5	0.03 ± 0.09	-0.09 ± 0.47	-0.13 ± 0.5	-36.72 ± 2.56	-65.47
plate-slide-back-side-v2-noise1	0.36 ± 0.31	0.37 ± 0.12	0.34 ± 0.18	-67.63 ± 20.56	-128.28
Average Relative Improvement	0.12	0.09	0.13	-	-
	Sigmoid	Rank	Constant	IQL	BC
assembly-v2-noise0.1	0.02 ± 0.07	-0.01 ± 0.04	-0.0 ± 0.04	-72.06 ± 2.34	-71.76
assembly-v2-noise0.5	-0.01 ± 0.01	-0.01 ± 0.02	0.01 ± 0.04	-122.97 ± 6.12	-129.53
assembly-v2-noise1	-0.01 ± 0.0	-0.01 ± 0.03	0.0 ± 0.03	-129.01 ± 1.62	-138.63
handle-press-side-v2-noise0.1	-0.05 ± 0.01	-0.05 ± 0.01	-0.05 ± 0.02	-34.1 ± 1.55	-36.28
handle-press-side-v2-noise0.5	0.06 ± 0.06	0.05 ± 0.07	0.07 ± 0.04	-37.28 ± 0.25	-34.3
handle-press-side-v2-noise1	-0.0 ± 0.11	0.03 ± 0.03	0.02 ± 0.07	-46.31 ± 3.11	-35.72
plate-slide-back-side-v2-noise0.1	0.01 ± 0.02	-0.01 ± 0.01	0.01 ± 0.03	-34.4 ± 1.23	-37.75
plate-slide-back-side-v2-noise0.5	0.07 ± 0.1	0.04 ± 0.08	0.03 ± 0.08	-34.03 ± 1.83	-65.47
plate-slide-back-side-v2-noise1	0.05 ± 0.18	0.01 ± 0.29	-0.04 ± 0.35	-43.95 ± 10.29	-128.28
Average Relative Improvement	0.01	0.01	0.01	-	-
	Sigmoid	Rank	Constant	TD3+BC	BC
assembly-v2-noise0.1	0.01 ± 0.02	0.02 ± 0.03	-0.01 ± 0.03	-72.44 ± 6.03	-71.76
assembly-v2-noise0.5	0.0 ± 0.02	0.02 ± 0.02	0.02 ± 0.04	-131.62 ± 5.25	-129.53
assembly-v2-noise1	0.0 ± 0.0	0.01 ± 0.01	0.0 ± 0.01	-138.0 ± 1.0	-138.63
handle-press-side-v2-noise0.1	-0.07 ± 0.02	-0.05 ± 0.02	-0.05 ± 0.02	-35.0 ± 2.14	-36.28
handle-press-side-v2-noise0.5	0.08 ± 0.04	0.08 ± 0.03	0.07 ± 0.05	-40.24 ± 1.06	-34.3
handle-press-side-v2-noise1	0.08 ± 0.08	0.06 ± 0.08	0.13 ± 0.17	-52.22 ± 5.29	-35.72
plate-slide-back-side-v2-noise0.1	0.16 ± 0.06	0.09 ± 0.05	0.03 ± 0.05	-39.31 ± 1.52	-37.75
plate-slide-back-side-v2-noise0.5	0.17 ± 0.24	-0.1 ± 0.33	-0.07 ± 0.32	-40.17 ± 1.64	-65.47
plate-slide-back-side-v2-noise1	0.19 ± 0.35	0.35 ± 0.28	0.07 ± 0.24	-91.74 ± 31.24	-128.28
Average Relative Improvement	0.07	0.05	0.02	-	-

D.6 Extended Results for Absolute Improvement

We report the experiment results in absolute improvement of normalized score for D4RL and Meta-World.

Table 11: Normalized score improvement for HUBL and normalized scores of base methods on D4RL datasets.

	Sigmoid	Rank	Constant	ATAC	BC
halfcheetah-medium-expert-v2	2.13 ± 0.35	1.55 ± 0.96	1.76 ± 0.14	92.5 ± 0.73	45.83
halfcheetah-medium-replay-v2	0.43 ± 0.38	0.96 ± 0.27	1.04 ± 1.01	46.89 ± 0.25	37.73
halfcheetah-medium-v2	-0.05 ± 0.71	0.16 ± 0.25	0.85 ± 0.35	52.54 ± 0.63	42.92
hopper-medium-expert-v2	0.36 ± 0.03	0.44 ± 0.26	0.27 ± 0.1	111.04 ± 0.13	57.51
hopper-medium-replay-v2	0.01 ± 0.48	0.21 ± 0.77	0.26 ± 0.32	101.23 ± 0.59	32.22
hopper-medium-v2	0.44 ± 3.28	1.57 ± 6.09	-2.35 ± 12.85	85.59 ± 4.76	53.81
walker2d-medium-expert-v2	0.08 ± 0.4	1.72 ± 0.5	0.26 ± 0.6	111.99 ± 0.8	105.3
walker2d-medium-replay-v2	2.76 ± 2.23	7.15 ± 0.31	4.38 ± 6.53	84.22 ± 2.7	22.78
walker2d-medium-v2	0.6 ± 0.5	-1.95 ± 4.62	1.35 ± 0.17	87.2 ± 0.67	64.18
Average Improvement	0.75	1.31	0.87	-	-
	Sigmoid	Rank	Constant	CQL	BC
halfcheetah-medium-expert-v2	1.55 ± 1.75	2.66 ± 4.77	-1.49 ± 13.59	81.96 ± 9.93	45.83
halfcheetah-medium-replay-v2	4.14 ± 0.22	7.19 ± 0.73	5.26 ± 0.4	40.98 ± 0.81	37.73
halfcheetah-medium-v2	-5.12 ± 0.43	-0.86 ± 0.72	-1.35 ± 0.68	51.05 ± 0.83	42.92
hopper-medium-expert-v2	32.62 ± 1.08	30.72 ± 5.21	29.5 ± 3.76	78.39 ± 14.51	57.51
hopper-medium-replay-v2	3.29 ± 0.79	0.69 ± 1.31	2.09 ± 0.75	97.21 ± 3.15	32.22
hopper-medium-v2	12.81 ± 10.16	10.87 ± 11.68	12.01 ± 4.51	70.27 ± 8.77	53.81
walker2d-medium-expert-v2	19.14 ± 0.42	19.74 ± 0.82	19.36 ± 0.14	89.38 ± 17.54	105.3
walker2d-medium-replay-v2	4.84 ± 17.24	24.07 ± 3.58	23.4 ± 2.24	63.35 ± 6.22	22.78
walker2d-medium-v2	3.62 ± 3.86	4.14 ± 2.23	-2.01 ± 11.8	79.41 ± 1.82	64.18
Average Improvement	8.54	11.02	9.64	-	-
	Sigmoid	Rank	Constant	IQL	BC
halfcheetah-medium-expert-v2	0.2 ± 0.9	-0.28 ± 0.19	-4.59 ± 2.6	92.92 ± 0.5	45.83
halfcheetah-medium-replay-v2	-1.51 ± 0.67	-0.08 ± 0.83	-1.86 ± 1.21	44.35 ± 0.21	37.73
halfcheetah-medium-v2	-0.28 ± 0.13	-0.06 ± 0.23	-0.68 ± 0.36	49.61 ± 0.16	42.92
hopper-medium-expert-v2	-4.52 ± 3.29	-2.88 ± 2.08	-10.22 ± 12.89	108.13 ± 2.69	57.51
hopper-medium-replay-v2	38.66 ± 4.79	31.57 ± 13.41	33.41 ± 14.48	53.98 ± 4.18	32.22
hopper-medium-v2	1.78 ± 2.05	1.27 ± 1.69	-0.68 ± 8.99	61.03 ± 3.27	53.81
walker2d-medium-expert-v2	1.53 ± 0.31	1.06 ± 1.01	0.99 ± 0.28	109.59 ± 0.2	105.3
walker2d-medium-replay-v2	10.78 ± 9.11	15.49 ± 1.61	9.2 ± 3.04	73.57 ± 2.64	22.78
walker2d-medium-v2	2.17 ± 1.46	2.54 ± 0.9	3.0 ± 0.71	81.68 ± 2.48	64.18
Average Improvement	5.42	5.4	3.17	-	-
	Sigmoid	Rank	Constant	TD3+BC	BC
halfcheetah-medium-expert-v2	-1.52 ± 2.92	-2.01 ± 2.51	-1.74 ± 2.29	94.82 ± 0.33	45.83
halfcheetah-medium-replay-v2	-5.48 ± 1.47	-4.41 ± 8.83	-0.24 ± 0.82	54.38 ± 1.24	37.73
halfcheetah-medium-v2	-4.28 ± 1.5	-2.85 ± 0.84	-0.76 ± 0.94	64.63 ± 2.15	42.92
hopper-medium-expert-v2	-5.8 ± 13.25	-15.45 ± 19.55	2.61 ± 4.79	98.79 ± 12.57	57.51
hopper-medium-replay-v2	13.36 ± 6.4	17.23 ± 2.15	19.7 ± 2.13	81.43 ± 27.77	32.22
hopper-medium-v2	30.06 ± 10.23	41.58 ± 1.11	35.2 ± 11.11	59.12 ± 3.39	53.81
walker2d-medium-expert-v2	0.36 ± 0.84	0.92 ± 0.95	0.53 ± 0.35	111.87 ± 0.17	105.3
walker2d-medium-replay-v2	9.85 ± 3.1	7.83 ± 5.66	3.86 ± 1.91	84.95 ± 1.85	22.78
walker2d-medium-v2	-0.75 ± 2.86	6.81 ± 1.13	0.37 ± 5.76	84.09 ± 1.94	64.18
Average Improvement	4.23	5.76	6.86	-	-

Table 12: Normalized score improvement for HUBL and normalized scores of base methods on MW datasets (part I)

	Sigmoid	Rank	Constant	ATAC	BC
button-press-v2-noise0.1	-0.09 ± 1.76	0.43 ± 0.62	0.41 ± 0.82	-58.12 ± 0.45	-58.79
button-press-v2-noise0.5	-0.21 ± 1.8	-2.22 ± 3.5	0.86 ± 2.75	-64.16 ± 0.93	-59.58
button-press-v2-noise1	-3.42 ± 4.41	-0.23 ± 2.71	-0.92 ± 2.28	-62.72 ± 3.84	-61.24
push-back-v2-noise0.1	8.81 ± 2.64	3.59 ± 6.53	12.75 ± 5.12	-87.12 ± 13.89	-104.85
push-back-v2-noise0.5	14.47 ± 8.88	25.88 ± 6.55	22.0 ± 3.23	-133.28 ± 14.24	-134.63
push-back-v2-noise1	5.38 ± 7.51	3.28 ± 12.83	7.94 ± 9.56	-141.29 ± 13.87	-143.63
reach-v2-noise0.1	-0.03 ± 1.08	-0.04 ± 0.9	0.0 ± 1.14	-17.19 ± 0.76	-18.31
reach-v2-noise0.5	12.53 ± 2.27	15.6 ± 1.9	14.49 ± 2.68	-33.91 ± 5.62	-24.57
reach-v2-noise1	18.22 ± 2.13	16.14 ± 11.32	23.09 ± 2.54	-46.58 ± 3.98	-43.79
Average Improvement	6.18	6.94	8.96	-	-
	Sigmoid	Rank	Constant	CQL	BC
button-press-v2-noise0.1	0.23 ± 1.96	1.32 ± 2.71	1.51 ± 1.87	-59.67 ± 1.69	-58.79
button-press-v2-noise0.5	-2.29 ± 2.67	-1.18 ± 0.55	-1.37 ± 0.19	-58.48 ± 0.85	-59.58
button-press-v2-noise1	-5.37 ± 7.82	5.46 ± 1.68	2.71 ± 7.2	-67.18 ± 14.25	-61.24
push-back-v2-noise0.1	-5.54 ± 5.79	1.54 ± 3.86	1.33 ± 1.89	-81.78 ± 2.88	-104.85
push-back-v2-noise0.5	30.82 ± 14.6	27.34 ± 12.97	23.15 ± 14.97	-124.64 ± 2.45	-134.63
push-back-v2-noise1	7.69 ± 16.81	14.41 ± 19.38	13.58 ± 7.12	-133.66 ± 8.17	-143.63
reach-v2-noise0.1	-0.77 ± 3.1	-0.22 ± 0.98	-0.67 ± 0.41	-18.5 ± 2.52	-18.31
reach-v2-noise0.5	21.05 ± 1.89	7.28 ± 21.76	16.49 ± 11.16	-41.02 ± 18.79	-24.57
reach-v2-noise1	86.19 ± 2.49	37.15 ± 15.77	86.65 ± 3.53	-107.14 ± 32.75	-43.79
Average Improvement	14.67	10.34	15.93	-	-
	Sigmoid	Rank	Constant	IQL	bc
button-press-v2-noise0.1	0.53 ± 0.6	1.87 ± 0.75	1.83 ± 0.58	-59.87 ± 1.32	-58.79
button-press-v2-noise0.5	-1.09 ± 1.25	-0.63 ± 1.16	-8.45 ± 7.68	-60.68 ± 0.29	-59.58
button-press-v2-noise1	-1.61 ± 8.16	5.17 ± 0.72	3.19 ± 2.58	-73.96 ± 5.09	-61.24
push-back-v2-noise0.1	2.93 ± 3.28	3.11 ± 1.89	2.47 ± 0.59	-83.79 ± 5.45	-104.85
push-back-v2-noise0.5	0.39 ± 11.3	4.62 ± 6.24	-4.16 ± 6.09	-124.86 ± 7.45	-134.63
push-back-v2-noise1	1.82 ± 5.35	3.71 ± 5.69	-0.35 ± 3.1	-143.26 ± 6.31	-143.63
reach-v2-noise0.1	-0.55 ± 0.2	-1.0 ± 0.45	-0.68 ± 1.23	-17.37 ± 0.87	-18.31
reach-v2-noise0.5	-2.48 ± 4.95	-0.58 ± 0.95	-0.58 ± 7.66	-31.51 ± 9.39	-24.57
reach-v2-noise1	-3.69 ± 5.46	2.12 ± 4.0	0.33 ± 15.48	-42.23 ± 7.4	-43.79
Average Relative Improvement	-0.41	2.04	-0.71	-	-
	Sigmoid	Rank	Constant	TD3+BC	BC
button-press-v2-noise0.1	19.12 ± 0.22	18.19 ± 0.17	18.01 ± 1.73	-77.68 ± 22.14	-58.79
button-press-v2-noise0.5	-2.47 ± 2.73	-2.11 ± 3.75	-5.36 ± 4.18	-59.54 ± 1.68	-59.58
button-press-v2-noise1	1.71 ± 5.97	9.71 ± 18.76	8.4 ± 9.47	-81.03 ± 5.79	-61.24
push-back-v2-noise0.1	7.18 ± 0.66	-1.06 ± 1.65	4.11 ± 3.08	-85.44 ± 5.05	-104.85
push-back-v2-noise0.5	9.43 ± 8.7	6.1 ± 17.6	6.43 ± 12.98	-127.95 ± 9.82	-134.63
push-back-v2-noise1	1.26 ± 6.0	1.4 ± 8.05	-5.31 ± 2.35	-139.72 ± 15.6	-143.63
reach-v2-noise0.1	-0.99 ± 0.66	-0.28 ± 0.31	-0.07 ± 0.38	-17.11 ± 1.28	-18.31
reach-v2-noise0.5	5.04 ± 7.92	10.2 ± 5.67	6.07 ± 7.23	-40.69 ± 9.66	-24.57
reach-v2-noise1	8.4 ± 12.06	2.34 ± 7.98	6.74 ± 7.36	-65.48 ± 2.85	-43.79
Average Improvement	5.41	4.94	4.34	-	-

Table 13: Normalized score improvement for HUBL and normalized scores of base methods on MW datasets (part II)

	Sigmoid	Rank	Constant	ATAC	BC
assembly-v2-noise0.1	-0.99 ± 2.28	1.0 ± 2.73	-0.23 ± 5.65	-70.22 ± 4.61	-71.76
assembly-v2-noise0.5	1.05 ± 2.43	3.59 ± 3.02	11.13 ± 6.31	-135.77 ± 1.58	-129.53
assembly-v2-noise1	-1.29 ± 1.99	2.47 ± 1.95	5.75 ± 1.07	-140.12 ± 2.45	-138.63
handle-press-side-v2-noise0.1	-0.93 ± 0.41	-0.49 ± 0.64	-0.88 ± 1.06	-32.38 ± 0.64	-36.28
handle-press-side-v2-noise0.5	0.08 ± 0.86	0.74 ± 0.94	-0.35 ± 1.06	-33.04 ± 0.96	-34.3
handle-press-side-v2-noise1	1.25 ± 4.2	-0.73 ± 3.55	-3.07 ± 2.05	-35.33 ± 3.7	-35.72
plate-slide-back-side-v2-noise0.1	-0.07 ± 1.44	-0.98 ± 0.82	0.77 ± 1.96	-37.07 ± 0.87	-37.75
plate-slide-back-side-v2-noise0.5	5.15 ± 28.23	11.72 ± 20.14	10.47 ± 1.41	-68.9 ± 10.92	-65.47
plate-slide-back-side-v2-noise1	16.4 ± 29.75	42.45 ± 2.22	43.25 ± 10.94	-97.9 ± 25.46	-128.28
Average Relative Improvement	2.29	6.64	7.43	-	-
	Sigmoid	Rank	Constant	CQL	BC
assembly-v2-noise0.1	2.37 ± 4.62	4.2 ± 12.62	4.36 ± 5.55	-76.29 ± 9.41	-71.76
assembly-v2-noise0.5	-0.57 ± 2.09	1.44 ± 5.55	-1.21 ± 2.87	-131.35 ± 2.62	-129.53
assembly-v2-noise1	-0.01 ± 3.97	-0.35 ± 2.07	0.56 ± 2.56	-138.94 ± 0.97	-138.63
handle-press-side-v2-noise0.1	3.79 ± 2.52	-0.53 ± 2.53	0.73 ± 6.56	-34.47 ± 4.54	-36.28
handle-press-side-v2-noise0.5	23.05 ± 7.99	26.8 ± 8.13	32.31 ± 0.94	-70.96 ± 29.39	-34.3
handle-press-side-v2-noise1	8.33 ± 6.37	6.94 ± 10.92	22.01 ± 2.89	-55.3 ± 33.42	-35.72
plate-slide-back-side-v2-noise0.1	1.83 ± 1.21	-0.02 ± 3.82	0.95 ± 3.95	-36.31 ± 2.33	-37.75
plate-slide-back-side-v2-noise0.5	0.96 ± 3.25	-3.16 ± 17.37	-4.94 ± 18.35	-36.72 ± 2.56	-65.47
plate-slide-back-side-v2-noise1	24.46 ± 21.13	24.72 ± 8.42	23.04 ± 12.37	-67.63 ± 20.56	-128.28
Average Relative Improvement	7.14	6.67	8.65	-	-
	Sigmoid	Rank	Constant	IQL	BC
assembly-v2-noise0.1	1.18 ± 4.78	-0.49 ± 3.07	-0.02 ± 3.2	-72.06 ± 2.34	-71.76
assembly-v2-noise0.5	-1.49 ± 1.27	-0.9 ± 1.89	1.13 ± 4.46	-122.97 ± 6.12	-129.53
assembly-v2-noise1	-1.31 ± 0.33	-0.76 ± 3.55	0.39 ± 3.85	-129.01 ± 1.62	-138.63
handle-press-side-v2-noise0.1	-1.56 ± 0.5	-1.67 ± 0.39	-1.66 ± 0.53	-34.1 ± 1.55	-36.28
handle-press-side-v2-noise0.5	2.16 ± 2.07	2.04 ± 2.46	2.56 ± 1.54	-37.28 ± 0.25	-34.3
handle-press-side-v2-noise1	-0.2 ± 5.06	1.33 ± 1.52	1.12 ± 3.27	-46.31 ± 3.11	-35.72
plate-slide-back-side-v2-noise0.1	0.24 ± 0.76	-0.18 ± 0.48	0.42 ± 1.12	-34.4 ± 1.23	-37.75
plate-slide-back-side-v2-noise0.5	2.3 ± 3.47	1.3 ± 2.69	0.92 ± 2.7	-34.03 ± 1.83	-65.47
plate-slide-back-side-v2-noise1	2.33 ± 7.7	0.63 ± 12.54	-1.8 ± 15.22	-43.95 ± 10.29	-128.28
Average Relative Improvement	0.41	0.14	0.34	-	-
	Sigmoid	Rank	Constant	TD3+BC	BC
assembly-v2-noise0.1	1.08 ± 1.69	1.16 ± 2.35	-0.71 ± 1.95	-72.44 ± 6.03	-71.76
assembly-v2-noise0.5	0.56 ± 3.01	2.16 ± 3.05	2.6 ± 5.8	-131.62 ± 5.25	-129.53
assembly-v2-noise1	0.48 ± 0.6	0.71 ± 1.39	0.03 ± 1.92	-138.0 ± 1.0	-138.63
handle-press-side-v2-noise0.1	-2.34 ± 0.77	-1.91 ± 0.87	-1.67 ± 0.69	-35.0 ± 2.14	-36.28
handle-press-side-v2-noise0.5	3.25 ± 1.66	3.17 ± 1.04	2.97 ± 1.82	-40.24 ± 1.06	-34.3
handle-press-side-v2-noise1	4.31 ± 4.29	3.39 ± 3.97	6.93 ± 8.89	-52.22 ± 5.29	-35.72
plate-slide-back-side-v2-noise0.1	6.11 ± 2.3	3.67 ± 1.77	1.09 ± 2.11	-39.31 ± 1.52	-37.75
plate-slide-back-side-v2-noise0.5	6.77 ± 9.5	-4.01 ± 13.35	-2.91 ± 13.02	-40.17 ± 1.64	-65.47
plate-slide-back-side-v2-noise1	17.06 ± 32.1	31.78 ± 25.94	6.48 ± 22.36	-91.74 ± 31.24	-128.28
Average Relative Improvement	4.14	4.46	1.65	-	-